Clim. Past Discuss., 6, 711–765, 2010
www.clim-past-discuss.net/6/711/2010/
doi:10.5194/cpd-6-711-2010

Climate of the Past Discussions

Evaluating climate model performance with various parameter sets using observations over the last centuries

M. F. Loutre[1], A. Mouchet[2], T. Fichefet[1], H. Goosse[1], H. Goelzer[3], and P. Huybrechts[3]

[1]Université catholique de Louvain, Earth and Life Institute, Georges Lemaître Centre for Earth and Climate Research (TECLIM), 2, Chemin du Cyclotron, 1348 Louvain-la-Neuve, Belgium
[2]Laboratoire de Physique Atmosphérique et Planétaire, Université de Liège, Allée du 6 août, 17, Bâtiment B5c, 4000 Liège, Belgium
[3]Earth System Science & Departement Geografie, Vrije Universiteit Brussel, Pleinlaan, 2, 1050 Brussels, Belgium

Received: 6 April 2010 – Accepted: 10 April 2010 – Published: 29 April 2010

Correspondence to: M. F. Loutre (marie-france.loutre@uclouvain.be)

Published by Copernicus Publications on behalf of the European Geosciences Union.

Abstract

Many sources of uncertainties limit the accuracy and precision of climate projections. Here, we focus on the parameter uncertainty, i.e. the imperfect knowledge of the values of many physical parameters in a climate model. We use LOVECLIM, a global three-dimensional Earth system model of intermediate complexity and vary several parameters within their range of uncertainty. Nine climatic parameter sets and three carbon cycle parameter sets are identified. They all yield present climate simulations coherent with observations and they cover a wide range of climate responses to doubled atmospheric CO_2 concentration and freshwater flux in the North Atlantic sensitivity experiments. They also simulate a large range of atmospheric CO_2 concentrations in response to prescribed emissions. Climate simulations of the last millennium are performed with the 27 combinations of these parameter sets. A special attention is given to the ability of LOVECLIM to reproduce the evolution of several climate variables over the last few decades, for which observations are available. The model response, even its ocean component, is strongly dominated by the model sensitivity to an increase in atmospheric CO_2 concentration but much slightly by its sensitivity to freshwater flux in the North Atlantic. The whole set of parameter sets leads to a wide range of simulated climates. Although only some parameter sets yield simulations that reproduce the observed key variables of the climate system over the last decades, all of them could be used to characterise extreme climate projections.

1 Introduction

Policymakers are facing a wide range of possible scenarios for long-term climate and sea level evolutions without knowing precisely why they differ and how reliable they are (e.g. IPCC, 2007; Knutti et al., 2008; Stainforth et al., 2007). There are indeed many sources of uncertainties in modelling experiments used in climate projections. Amongst others, there are uncertainties in the future anthropogenic emissions of greenhouse gases and aerosols (e.g. Nakicenovic and Swart, 2000; Meehl et al., 2007), and uncertainties in the boundary and initial conditions (e.g. Knutti et al., 2008). Moreover, climate models, and in particular the physical parameterisations they are using, are far from being perfect and the values of many physical parameters themselves are often poorly known (e.g. Stainforth et al., 2005; Murphy et al., 2004).

Several strategies can be used to assess those uncertainties. Model results can be analysed to quantify some of the uncertainties related with the models themselves. For example, Gleckler et al. (2008) proposed objective measures of climate model performance. They used their metric to assess General Circulation Model (GCM) simulations of the last century climate performed within the Coupled Model Intercomparison Project (CMIP3). In parallel, the modelled responses to different external forcings are utilised to illustrate the uncertainty related with the non-perfect knowledge of the forcing (e.g. Crowley, 2000; Bertrand et al., 2002). Furthermore, Murphy et al. (2004) and Stainforth et al. (2005) used the same model and the same forcings with varied values of key physical parameters to identify the range of the climate response to a CO_2 doubling related with parameter uncertainty. Based on several emission scenarios and coupled GCMs, Knutti et al. (2008) concluded that the contribution of structural uncertainties (i.e. the error related with the choices made in the model structure that would remain even if all the parameters were perfectly known) to temperature projection over the next century is quite large.

Among all those possible sources of uncertainty, we focus here on the parameter uncertainty. More specifically, the overall goal of this study is to identify a reasonable number of parameter sets in LOVECLIM, a global three-dimensional Earth system model of intermediate complexity (Goosse et al., 2010), each parameter within its range of uncertainty, that yield past and present climate simulations coherent with observations. Furthermore, all the parameter sets should lead to a range of possible climate and sea level change scenarios over the next millennia in order to provide a reasonable sample of uncertainty of future changes, uncertainty that will be analysed in forthcoming studies. This approach has been chosen rather than a systematic random variation of all

CPD
6, 711–765, 2010

the important parameters because the latter would imply a very large number of long simulations, which is not affordable even with a relatively fast model like LOVECLIM. Moreover, preliminary tests clearly showed that most parameter combinations lead to unrealistic present-day climate and therefore would be useless for the purpose of this study. In addition, using a restricted number of parameter sets allows a better knowledge of their characteristics and thus potentially offers a better understanding of the different responses.

First, we identify 27 combinations of key physical parameter values of LOVECLIM that have a large impact on the model results. Three types of experiments are conducted to test model behaviour using those parameters. A control experiment under pre-industrial conditions is performed to ensure that all the selected parameter sets yield a reasonable pre-industrial climate. A freshwater hosing experiment (to assess the stability of the North Atlantic Meridional Overturning Circulation, MOC) and an experiment in which the CO_2 concentration is doubled (to provide a clear and strong climate signal) allow the quantification of the range of climate response. The very classical doubled CO_2 and water hosing experiments are chosen because they provide a good insight into the response of the atmosphere and ocean under perturbed conditions. Furthermore, the response of LOVECLIM can be compared to the one of other models in similar conditions (e.g. Rahmstorf et al., 2005; Brovkin et al., 2006; Weber et al., 2007). The last experiment is mainly devoted to the analysis of the carbon cycle as discussed below

Second, the selected parameter sets are utilised to carry out transient experiments over the last millennium to ensure that each parameter set is able to reproduce adequately past climate variability and changes on that time-scale. More precisely, we intend to identify those that are the most appropriate to simulate past climate. In this paper, we show that all the selected parameter sets are able to reproduce the major global features of the climate evolution over the pre-industrial period. Therefore, we further focus on the ability of the model to simulate the trend of key climate variables over the last century. This time interval also corresponds with a period when more accurate

CPD
6, 711–765, 2010

reconstructions and observations are available for model comparison. Finally, a metric (i.e. a scalar measure) is designed to quantify this ability.

The LOVECLIM model is described in Sect. 2. The parameter sets are selected in Sect. 3. The responses to a doubled CO_2 concentration and to a freshwater perturbation are analysed in Sect. 4 along with the present-day climate and the sensitivity of the carbon cycle according to the different parameter sets. Major features of the simulated climate over the last millennium are described in Sect. 5, while a special emphasis is given on the last century in Sect. 6. At last, the metric used to quantify the skill of the different parameter sets in simulating climate trend over the last century is presented in Sect. 7.

2 Model description

LOVECLIM1.1 (further termed LOVECLIM) is a three-dimensional Earth System Model of Intermediate Complexity (EMIC). It consists of five components representing the atmosphere (ECBilt), the ocean and sea ice (CLIO), the terrestrial biosphere (VECODE), the oceanic carbon cycle (LOCH) and the Greenland and Antarctic ice sheets (AGISM). The ice sheet model AGISM (Huybrechts, 1990, 1996; Huybrechts and de Wolde, 1999) is not activated in this study because of the negligible influence of ice sheet-climate interactions on the climate evolution over the last millennium. Rather, its influence on future climate simulations is investigated in a separate study (Goelzer et al., 2010). The previous model version (LOVECLIM1.0) is described in Driesschaert et al. (2007), while version 1.2, which differs only very slightly from version 1.1, is presented in Goosse et al. (2010).

ECBilt (Opsteegh, 1998) is a quasi-geostrophic atmospheric model with 3 levels and T21 horizontal resolution that explicitly computes synoptic variability associated with weather patterns. It includes simple parameterisations of the diabatic heating processes and an explicit representation of the hydrological cycle. Cloudiness is prescribed according to present-day climatology, which is a limitation of the present study.

CPD
6, 711–765, 2010
Climate model performance over the last centuries
M. F. Loutre et al.

CLIO (Goosse and Fichefet, 1999) is a primitive-equation, free-surface OGCM coupled to a thermodynamic-dynamic sea ice model. Its horizontal resolution is 3°×3°, and there are 20 levels in the ocean. VECODE (Brovkin et al., 2002) is a reduced-form model of vegetation dynamics and of the terrestrial carbon cycle. It simulates the dynamics of two plant functional types (trees and grassland) at the same resolution as that of ECBILT. LOCH (Mouchet and François, 1996; Mouchet, 2010) is a comprehensive oceanic carbon cycle model that includes an atmospheric module to represent the evolution of CO_2, $^{13}CO_2$ and $^{14}CO_2$ in the atmosphere. LOCH is fully coupled to CLIO and runs with the same time step and on the same grid. LOVECLIM has been utilised in a large number of climate studies (e.g. Driesschaert et al., 2007; Goosse et al., 2007; Menviel et al., 2008a, 2008b) and was part of several model intercomparison exercises (e.g. Braconnot et al., 2002, 2007a, 2007b; Dutay et al., 2004).

3 The parameter sets

3.1 Climatic parameters

Several physical parameters of the model may significantly impact the model response to an external perturbation. We use expert judgment to select sensitive ones. Although other studies (Collins et al., 2007; Brierley et al., 2010) suggested that the impacts of ocean parameter uncertainty on climate response is small compared to perturbed atmosphere parameters, the parameters are selected in both the atmospheric (ECBilt) and oceanic (CLIO) components of the model. The parameter sets are chosen to produce reasonable simulations of the present-day climate and to lead to contrasted responses to a doubling of CO_2 concentration and to additional freshwater flux in the North Atlantic. The parameter values are chosen within their range of uncertainty. In doing so, we want to keep a grip on the parameter sets in order to be able to identify the impact of each configuration on the simulated climate. This is also why the number of parameter sets included in this study is relatively small. Table 1 gives the values for the nine selected climatic parameter sets. Parameter sets E11, E21, E31, E41, and E51 were previously used by Goosse et al. (2007). We present a short description of those parameters in Table 1. The Rayleigh damping term of the equation of the quasi-geostrophic potential vorticity includes two parameters. The first one, $\lambda 2$, corresponds to the 200–500 hPa layer of the model, while the second one, $\lambda 4$, corresponds the 500–800 hPa layer (see Eq. 1 of Opsteegh et al., 1998, and Eq. 11 of Haarsma et al., 1996).

The simple longwave radiative scheme of LOVECLIM is based on an approach termed the Green's function method (Chou and Neelin, 1996; Schaeffer et al., 1998). The scheme could be briefly represented for clear-sky conditions by the following formula for all the model levels:

$$F_{\mathrm{lw}} = F_{\mathrm{ref}} + \mathrm{FG}\left(T', \mathrm{GHG}'\right) + G1 \cdot \mathrm{amplw} \cdot (q')^{\mathrm{explw}}$$

where F_{lw} is the longwave radiation, F_{ref} a reference value of the radiation when temperature, humidity and the concentration of greenhouse gases are equal to the reference values, and FG a function, not explicitly described here, allowing to compute the contribution associated with the anomalies compared to this reference in the vertical profile of temperature (T') and in the concentrations of the various greenhouse gases in the atmosphere (GHG'). The last term represents the anomaly in the longwave radiation due to the anomaly in humidity q'. The coefficients F_{ref}, $G1$ and those included in the function FG are spatially dependent. All the terms have been calibrated to follow as closely as possible a complex GCM longwave radiative scheme (Schaeffer et al., 1998), but large uncertainties are of course related to this parameterisation, in particular as the model only computes one mean relative humidity between the surface and 500 hPa, the atmosphere above 500 hPa being supposed to be completely dry. Here, both amplw and explw are varied with a clear impact on the influence of humidity changes on long wave fluxes.

The albedo of the ocean in LOVECLIM depends on the season and location. At each time step, it is multiplied by albcoef. For a typical albedo of the ocean of 0.06, using a value of 1.05 for albcoef increases the value of the albedo to 0.063.

CPD
6, 711–765, 2010

The albedo of sea ice (albice) is computed by the scheme of Shine and Henderson-Sellers (1985), which uses different values for the albedo of snow, melting snow, bare ice and melting ice. For thin ice, the albedo is also dependent on the ice thickness. If albice is different from zero in the experiments discussed here, the value of the albedo in the model is increased by albice for all the snow and ice types.

The minimum vertical diffusion coefficient in the ocean follows a vertical profile similar to the one proposed by Bryan and Lewis (1979), as explained in detail in Goosse et al. (1999). The coefficient avkb is a scaling factor that multiplies the minimum values of the vertical diffusion at all depths. A value of avkb of 1 (1.5, 2, 2.5) corresponds to a minimum background vertical diffusivity in the thermocline of 10^{-5} m^2/s (1.5×10^{-5}, 2.0×10^{-5}, 2.5×10^{-5} m^2/s).

The semi-implicit numerical scheme used for the Coriolis term in the barotropic and baroclinic horizontal momentum equation in LOVECLIM1.0 (Driesschaert et al., 2007) induced too much numerical noise. Therefore, in LOVECLIM1.1, it is computed in a totally implicit way for all the simulations, except those using the E11 climatic parameter set. The former scheme is kept here in these experiments E11 in order to provide an easier comparison with the results of LOVECLIM1.0. Because of the larger implicit diffusion associated with this scheme, a lower value of the explicit diffusion is applied in E11.

As ECBilt systematically overestimates precipitation over the Atlantic and Arctic Oceans, it has been necessary to artificially reduce the precipitation rate over the Atlantic and Arctic basins (defined here as the oceanic area north of 68° N). The corresponding water is dumped into the North Pacific, a region where the model precipitation is too weak (Goosse et al., 2001). CorA corresponds to the percentage of reduction of the precipitation in the Atlantic.

3.2 The carbon cycle parameters

In addition to the nine climatic parameter sets (based on the parameters) described in the previous section, we define three parameter sets inducing different responses of

Discussion Paper | Discussion Paper | Discussion Paper | Discussion Paper |

CPD

6, 711–765, 2010

Climate model performance over the last centuries

M. F. Loutre et al.

the carbon cycle model (i.e. carbon parameter sets; Table 2). The key parameters for the carbon cycle are chosen among those which have a strong impact on the marine biogeochemical cycle and on the response of atmospheric CO_2 to emission scenario. More precisely, they deal with the continental vegetation fertilization effect, on the one hand, and the rain ratio and the vertical flux of particulate organic matter (POM) in the ocean, on the other hand (Table 2) (Mouchet, 2010).

The fertilization effect constitutes a negative feedback on CO_2. The effect of CO_2 on continental vegetation uptake is parameterised with the following formula:

$$\mathrm{NPP} = \mathrm{NPP0}\left(1+\beta \ln\left(p\mathrm{CO}_2/p\mathrm{CO}_{2\mathrm{ref}}\right)\right),$$

where NPP is the net primary production, $p\mathrm{CO}_2$ the CO_2 atmospheric pressure, and NPP0 and $p\mathrm{CO}_{2\mathrm{ref}}$ the NPP and $p\mathrm{CO}_2$ for a reference state, respectively. As there are different fertilization responses according to the ecosystem (e.g. Houghton et al., 2001), we separated the fertilization effect in two terms: one for grass (βg) and one for forests (βt).

The vertical flux of POM is one factor controlling the sequestration of CO_2 in the deep ocean. It is represented in the model by a power law z^{α} with z the depth (Martin et al., 1987). The α factor exhibits a large range of values (e.g. Martin et al., 1987; Suess, 1980; Berger et al., 1987; Betzer et al., 1984). Such a range could be explained by differences in ecosystems (e.g. Klaas and Archer, 2002). Hence carbon parameter set 1 considers different profiles for diatoms (α_{diatom}) and other species (α_{others}) in order to account for the sensitivity of α on ecosystem composition.

The buildup of calcium carbonate shells in the surface ocean results in a CO_2 source to the atmosphere, while dissolution constitutes a sink. The Ψ_{zoo} parameter represents the contribution of zooplankton in the precipitation of biogenic $CaCO_3$. A larger value of this parameter implies a larger rain ratio. The rain ratio is defined as the ratio of inorganic carbon content over that of organic carbon in biogenic particles sinking to depth.

CPD
6, 711–765, 2010

4 Preliminary experiments

4.1 The pre-industrial climate

An equilibrium experiment, under pre-industrial conditions, is performed using each of the nine selected climatic parameter sets. For these simulations, LOVECLIM is coupled neither with the ice sheet model (AGISM) nor the oceanic carbon cycle model (LOCH). The various forcings are kept constant. No volcanic eruption is considered. The greenhouse gas concentrations are kept to their 1750 values (all years are in AD). Simulated climatic variables are compared to recent observations. Pre-industrial and present-day climates are slightly different. Actually, the model-data comparison mostly put forward the systematic biases of the model that are present with almost all parameter sets (e.g. Fig. 1) as well as in other versions of the model (Goosse et al., 2001, 2010). However, our purpose here is to demonstrate that all the parameter sets lead to reasonable mean states but not to analyse in detail model performance for the mean climate, as explained in the introduction. This difference between recent and pre-industrial climates is thus of minor importance in the present study.

Table 3 displays some global features simulated by LOVECLIM using the different parameter sets under pre-industrial forcing. For all the parameter sets, the globally averaged annual mean surface temperature is slightly too high, varying between 15.8 and 16.4 °C, the main overestimation being observed at low latitudes (Fig. 1a). LOVECLIM underestimates precipitation in the equatorial region (Fig. 1b). This model feature is a consequence of the quasi-geostrophic approximation, which induces difficulties to simulate a correct Hadley cell (Renssen et al., 2002); it is not significantly modified by any parameter set. Mid- and high-latitude precipitation is more properly represented than equatorial precipitation, independent of the parameter set. The model overestimates the tree fraction (Fig. 1c) at all latitudes, whatever the parameter set. This overestimation is mostly at the expanses of the grass fraction, except in the mid-to-high southern latitudes (southern South America), where the cold desert area is underestimated. This

CPD
6, 711–765, 2010

general feature of the model is related with the overestimation of temperature over land, which is in favour of tree growth. The maximum of the strength of North Atlantic MOC (i.e. the annual mean value of the maximum of the North Atlantic meridional overturning streamfunction below the Ekman layer) varies between 17 and 28 Sv. These values lie within the range given by GCMs (e.g. Dixon and Lanzante, 1999; Gent, 2001). The sea ice extent in the Northern Hemisphere varies seasonally from a maximum between 14.3 and 15.1×10^6 km^2 in March to a minimum between 6.7 and 9.3×10^6 km^2 in September, while observations (average value between 1979 and 2000; Comiso and Nishio, 2008) give a maximum of less than 16×10^6 km^2 and a minimum of 6.9×10^6 km^2.

4.2 Sensitivity to CO_2 concentration

A first sensitivity experiment is performed starting from the equilibrium state described in the previous section. The atmospheric CO_2 concentration is enhanced by 1% per year from the pre-industrial value until a doubled value is reached, i.e. after 70 years. It is held constant thereafter (Fig. 2, left). The increase in global annual mean surface temperature after 1000 years in this sensitivity experiment is chosen as an index to characterise the response of the model to the prescribed perturbation (CO_2 sensitivity).

The global annual mean surface temperature increase for the 9 climatic parameter sets ranges from 1.7 to 4.0 °C after 1000 years (Table 3). Although model E11 is not exactly the same as LOVECLIM1.0 used in Driesschaert et al. (2007), it shares many climatic features with this former version. In particular, its CO_2 sensitivity is rather low, i.e. 1.7 °C. Figure 2 (right) displays the temperature evolution during the first 1000 years of the experiment. The rate of change is largest over the first 70 years of the simulation, when atmospheric CO_2 concentration is increasing. However, a new equilibrium is not yet reached after 1000 years with all the parameter sets.

The name of the experiments (e.g. first column in Tables 1 and 3) has been designed to provide a quick overview of their main characteristics. Indeed, the first digit is related to the CO_2 sensitivity. Its value goes from 1 to 5, corresponding to an increase less than

CPD
6, 711–765, 2010

2.0 °C to more than 3.5 °C (by step of 0.5 °C) in global annual mean surface temperature after 1000 years in the experiment described above (Fig. 2).

4.3 Sensitivity to water hosing

In a second sensitivity experiment an anomalous amount of freshwater is added in the North Atlantic (20°–50° N) with a linearly increasing rate of 2×10^{-4} Sv/yr during 1500 years. This results in a freshwater perturbation of 0.1 Sv after 500 years, 0.2 Sv after 1000 years, and 0.3 Sv after 1500 years (Fig. 3, left). The percentage of decrease of the maximum value of the meridional overturning streamfunction below the Ekman layer in the Atlantic Ocean after 1000 years in this water hosing experiment (at the time the perturbation reaches 0.2 Sv) is chosen to characterise the response of the model to this perturbation (MOC sensitivity). Model E11, i.e. the closest configuration to the one used in Driesschaert et al. (2007), simulates a 16% reduction in the meridional overturning streamfunction after 1000 years. This decrease ranges from 16 to 57% for the other parameter sets (Table 3).

The MOC sensitivity is reflected in the second digit of the name of the experiments. It is one or two according to whether the decrease in the meridional overturning streamfunction after 1000 years is smaller or larger than 50%.

It is worth reminding that the model parameter sets lead to different pre-industrial equilibrium states with respect to the MOC (Table 3). Moreover, the time evolution of the meridional overturning streamfunction during the water hosing experiment shows several different patterns according to the model parameter sets (Fig. 3, right). Indeed, for some model parameter sets (e.g., E11), the meridional overturning streamfunction decreases almost linearly, while for others (e.g., E12), the MOC experiences a more abrupt weakening.

Figure 4 shows that the phase space (MOC sensitivity vs. CO_2 sensitivity) of our set of experiments is rather homogeneously covered as required by our initial objective. For comparison, the GCMs used in the IPCC-AR4 (Randall et al., 2007) have an equilibrium CO_2 sensitivity ranging from 2.1 °C to 4.4 °C, with a mean value of 3.2 °C. Our parameter sets almost cover this range except for the largest CO_2 sensitivities. In an intercomparison of EMICs, Rahmstorf et al. (2005) showed that the width of the hysteresis curve, corresponding to changes in freshwater input, varies between 0.2 and 0.5 Sv. Amongst the models used in this intercomparison, those with three-dimensional ocean models (including ECBilt-CLIO, a former version of LOVECLIM, with general features similar to those of parameter set E11) display a sharp weakening of the North Atlantic MOC for a freshwater input of less than 0.3 Sv. In our sensitivity experiment, which uses a slightly different setup, the meridional overturning streamfunction displays a very strong reduction for freshwater input ranging from 0.2 Sv to 0.4 Sv.

4.4 Sensitivity of the carbon cycle

We assess the sensitivity of the atmospheric CO_2 level to the carbon parameter sets by performing a prognostic CO_2 experiment for each of these sets. This transient simulation starts from an equilibrium state corresponding to the conditions prevailing in 1750. It runs until 3000 and is constrained by changes in the Earth orbital parameters (Berger, 1978) and in concentrations of greenhouse gases (GHGs) except for CO_2. In addition the model is forced by anthropogenic emissions of CO_2, including both fossil fuel and deforestation fluxes. Over the historical period (1750–2000), the GHG concentrations (except for CO_2) (Houghton et al., 2001) and carbon emissions (Marland et al., 2003; Houghton, 2003) follow the historical records. From 2000 to 2100, we use the SRES A2 scenario (Houghton et al., 2001) for both carbon emissions and GHG concentrations. After 2100, concentrations of all GHGs (except for CO_2) are kept fixed to their 2100 values while CO_2 emissions from land use are set to zero and fossil fuel emissions decrease according to a bell-shaped curve so that they reach zero a few decades after 2200 (Fig. 5). In parallel, each experiment is accompanied with a control simulation in which all the forcings are maintained at their 1750 values with no anthropogenic CO_2 emission.

The three carbon parameter sets lead to contrasted responses of the atmospheric CO_2 to the identical forcing (Fig. 6a). Maximal values of the atmospheric CO_2

CPD
6, 711–765, 2010

concentration differ by up to 169 ppmv between carbon sets 1 and 3 (Fig. 6, Table 2). By year 2500, they still differ by 133 ppmv, i.e. a relative difference of about 11%. With parameter sets 1 and 2, the land CO_2 uptake outpaces the ocean uptake (Fig. 6b), while the reverse happens with carbon set 3.

The parameters related to the continental vegetation processes explain up to 87% of the difference in atmospheric CO_2 response between the various experiments. On such timescales, changes in the rain ratio or in the export production have a much smaller impact on the atmospheric CO_2. The contribution of the rain ratio to the maximum value of the atmospheric CO_2 range is about 10%, while changes in remineralization depth explain about three percents. Such small changes (a few ppmv) are within the variability produced by the model and cannot be ascertained yet. All together, the three parameter sets allow us to obtain a change in the carbon climate sensitivity (Frank et al., 2010) of the order of 7% (Fig. 6c).

The third digit in the experiment name refers to the carbon parameter set with relatively low (1), medium (2) or high (3) changes in atmospheric CO_2 in response to the same emission scenario.

5 Last millennium

The climate of the last millennium is simulated for each of the 27 parameter sets involving climate and carbon parameters. All the simulations start at year 500 from an equilibrium state at that time and are run in transient mode until year 2000. Two different methods are used for the evolution of the atmospheric CO_2 concentration, either diagnostic or prognostic. In the diagnostic mode (Conc), the atmospheric CO_2 concentrations are prescribed according to Antarctic records until 1750 (Flückiger et al., 2002; Monnin et al., 2004; Siegenthaler et al., 2005; Meure et al., 2006), according to Enting et al. (1994) between 1750 and 1990, and according to GLOBALVIEW-CO2 (2006) after 1990 (Fig. 7). For the prognostic mode (Efor), the atmospheric CO_2 concentration is computed by forcing the model with emissions of CO_2 from fossil fuel burning (Fig. 8;

Marland et al., 2003). Both simulations also take into account land use changes related with human activities as in Goosse et al. (2005) (percentage of crops; Ramankutty and Foley, 1999). The scenario of historical changes in global land cover developed by Ramankutty and Foley (1999) starts only in 1700. We hypothesize that the land cover changes evolved linearly from its natural state in 500 to the estimated values in 1700. Moreover, we assume that croplands replace only forests, as long as there is a forest fraction. Furthermore, desert and forest (except for the part replaced by crops) keep their original extent at year 500. This scenario was used in a model intercomparison exercise aiming at analysing the response of six EMICs, including ECBilt-CLIO-VECODE, to historical deforestation (Brovkin et al., 2006).

In addition to the atmospheric CO_2 concentration, either prescribed or computed by the model, the transient simulations are forced by the volcanic activity (Crowley, 2000), the solar activity (Muscheler et al., 2007), the Earth orbital parameter changes (Berger, 1978; Bretagnon, 1982) and changes in concentrations of GHGs other than CO_2 (Prather et al., 2001; Houghton et al., 1990, and updates). The effect of sulphate aerosols is accounted for through a modification in surface albedo, as suggested by Charlson et al. (1991).

The simulations reveal that all our parameter sets lead to a reasonable and stable climate on millennial timescales. Although none of the simulations is perfect, none of them is in complete disagreement with available climate observations (or reconstructions). As illustrated by the simulated NH surface temperature in Conc and the atmospheric CO_2 concentration simulated in Efor (Fig. 7), all simulations show relatively good agreement with reconstructions. Furthermore, this figure shows a strong consistency between all the simulations (and all the parameter sets) over the whole duration of the simulations. The comparison between simulated and reconstructed global variables representative of the climate evolution over the last millennium will not allow us to rank the ability of the parameter sets to properly simulate the climate evolution over the past millennium. Indeed the uncertainties in climate reconstructions over that timescale are large, and the variability of the model may prevent an accurate

CPD
6, 711–765, 2010

comparison. Therefore, we decided to focus on the most recent part of these simulations (i.e. the last century) for which some accurate measurements of climatic variables are available. This will allow a quantitative assessment of the agreement between simulations and observations.

6 Last century

6.1 The simulations

In this section, we study the model behaviour over the last century in the simulations using the different parameter sets. Our purpose is to quantify the ability of each parameter set to simulate climate changes over the last century, or over shorter periods, for which accurate observations are available. For the analysis of the simulated climate changes over the last millennium, we smoothed the global variables with a 31-yr window to reduce the variability. For the last century experiments, we consider the mean over an ensemble of five members in order to reduce the impact of internal variability. Each member consists in a simulation of the last century climate (1900–2010). The members of one ensemble differ only in their initial conditions. To do so, we have introduced a very small perturbation in the quasi-geostrophic potential vorticity the first day of the simulation, as done in Goosse et al. (2007). Each simulation starts in 1900 from the state of the corresponding millennium simulation at that time. The average of the members is analysed and discussed.

For 150 years human activities have increased the sulphate aerosol load in the troposphere (Houghton et al., 2001). However, the magnitude of its effect on Earth climate is difficult to estimate. The radiative forcing computed by LOVECLIM for the present day with respect to the pre-industrial era related to the sulphate aerosol load is –0.4 $\mathrm{W\,m^{-2}}$ in the reference situation (E11). However, there is a large uncertainty in this quantity. IPCC-AR4 (Forster et al., 2007) reported a direct radiative forcing due to sulphate aerosols of –0.40±0.2 $\mathrm{W\,m^{-2}}$. The overall aerosol direct radiative forcing

CPD
6, 711–765, 2010

(i.e. radiative forcing values associated with several aerosol components) was estimated to –0.50±0.40 Wm^{-2}. In addition to a direct effect, aerosol particles also affect the formation and properties of clouds. IPCC-AR4 gives a median value of –0.70 Wm^{-2} for the cloud albedo radiative forcing due to aerosol influence on clouds. Therefore, we decide to perform a second set of simulations for which the radiative forcing related to sulphates is doubled (S2).

This study concentrates on global climate features. Furthermore, LOVECLIM has been (and continues to be) mainly used in process studies focused on mean and high latitudes. Therefore, we have selected variables that potentially have a direct or indirect impact on the evolution of sea level, on the stability of the North Atlantic MOC, on the future of the climate of the polar regions, or, more generally speaking, on global climate change. In addition to atmospheric CO_2 concentration and surface temperature already presented in Sect. 5, we specifically assess the ability of the model to reproduce the observed trend in the Northern Hemisphere sea ice extent, and ocean heat content.

6.2 CO_2 concentration

The comparison of the simulated time evolution of the atmospheric CO_2 concentration over the last century with data shows that some parameter sets display a poorer agreement than others (Fig. 9). In particular, the simulated increase in CO_2 concentration obtained with carbon parameter set 3 is of the order of 10 ppmv larger than in the corresponding observations over the 20th century. By contrast, the simulated increase in atmospheric CO_2 concentration remains close to the measured one for carbon parameter sets 1 and 2.

Similar conclusions can be reached by analysing the rate of increase in CO_2 concentration over different periods. Between 1959 and 2008, it varies between 1.35 and 1.47 ppmv/yr, for carbon parameter sets 1 and 2, with the nominal (S1) sulphate forcing. Furthermore, the rate is higher with the carbon parameter set 3 (∼1.58 ppmv/yr) as well as when the S2 sulphate forcing is applied (by about 0.03 ppmv/yr). It is in reasonable agreement with the corresponding value in the Mauna Loa record (NOAA

CPD
6, 711–765, 2010

ESRL, 2009[1]) of 1.44 ppmv/yr. A comparison with another observation series (Enting et al., 1994; GLOBALVIEW-CO2, 2006) over the time interval 1979–2005 yields similar conclusions. For this period the rate of increase in CO_2 concentration varies between 1.48 and 1.62 ppmv/yr, for carbon parameter sets 1 and 2, with the S1 sulphate forcing. It is higher with the carbon parameter set 3 (between 1.71 and 1.79 ppmv/yr). Here we obtain a larger CO_2 increase for a smaller temperature increase, which can be considered as a negative CO_2-climate feedback. In other words, the net feedback (Friedlingstein et al., 2003), which is the global warming amplification, is slightly smaller than one.

On the other hand, compared to the Mauna Loa record (NOAA ESRL, 2009[1]), the absolute values of atmospheric CO_2 concentration between 1959 and 2008 are the best reproduced with carbon parameter set 3 when using the S1 sulphate forcing, and with carbon parameter sets 2 or 3, depending on the climate parameter set, when a higher sulphate concentration is used.

6.3 Surface temperature

The increasing trend in global annual mean surface temperature, computed from HadCRUT3 time series (Brohan et al., 2006) is 0.0168 °C/yr over the last 35 years (1979–2005) and 0.0071 °C/yr over the last century (1901–2005). Several parameter sets lead to an underestimate of this increasing trend. This is for example the case for 11, 21, and 22, especially with the S2 sulphate forcing, while other parameter sets yield overestimate of this trend, e.g. 51 and 52, especially with the S1 sulphate forcing. This behaviour was mostly expected due to differences in CO_2 sensitivity. Indeed, the parameter sets corresponding to the lowest CO_2 sensitivity (such as 11, 21, and 22) lead to small temperature changes over the last century and those with the largest sensitivity (e.g. 51 and 52) lead to a large temperature increase over the last century. Moreover, using a larger sulphate aerosol forcing tends to shift the simulated temperature

[1]www.esrl.noaa.gov/gmd/ccgg/trends/; last access: 13 July 2009

CPD
6, 711–765, 2010

increase over the last century towards smaller values because of the radiative cooling effect of those aerosols. Still, the discrepancy between simulated global annual mean surface temperature and observations remains small (within one standard deviation) for many configurations.

Moreover, although the deviation from observations of the simulated atmospheric CO_2 concentration is of the order of 10 ppmv over the 20th century (Fig. 9) for carbon parameter set 3, this discrepancy is not large enough to drive the surface temperature towards larger values than for carbon parameter set 1 or 2. Therefore, most of the simulations with carbon parameter set 1 or 2 remain close to temperature observations, while those using carbon parameter set 3 are slightly further.

6.4 Minimum sea ice extent

Most of the simulations, either with S1 or S2 sulphate aerosol forcing, experience a too small decrease in Northern Hemisphere minimum sea ice extent between 1979 and 2006 compared to observations (Fig. 10). This is especially the case for those simulations with low climate sensitivity (11, 12, 21, and 22). For higher sensitivities, the type of simulation (Efor or Conc), the sulphate aerosol load, as well as the sensitivity to the carbon cycle may play a role in the simulated trend. However, larger sulphate aerosol concentrations do not systematically lead to lower or higher trend in Northern Hemisphere minimum sea ice extent.

6.5 Oceanic variables

Most of the simulations overestimate the warming of the global ocean in the 700 m upper layer, over the last 50 years, when the S1 sulphate forcing is used (Fig. 11). This overestimation is strongly reduced for S2 sulphate forcing. Indeed, in that case only the simulations with high climate sensitivity (51, 52, as well as 32 and 41 for some configurations) simulate an ocean heat content increase significantly larger than in the real world.

CPD
6, 711–765, 2010

The modelled ocean circulation does not experience major changes during the last century. All the simulations exhibit a reduction of less than 4 Sv in the strength of North Atlantic MOC for S1 sulphate aerosol forcing [3 Sv; S2 sulphate aerosol forcing] over the last century (Fig. 12). It must be reminded that there is a large spread in the mean intensity of the MOC depending on the parameter sets. For example, this strength varies between 28 and 17 Sv in 1900 depending on the parameter set used.

In a model intercomparison, Gregory et al. (2005) used several GCMs and EMICs (including LOVECLIM) to study the response of the North Atlantic MOC to an increase in atmospheric CO_2 concentration. In this context, partially coupled integrations were performed to evaluate the influence of heat and freshwater in each of the models. They pointed out that heat flux changes contribute more than freshwater flux changes to weakening the MOC for all models.

The simulations performed here display an approximately linear relationship between the increase in the upper ocean heat content and the increase in sea surface temperature (Fig. 11), i.e. when temperature increases, in particular sea surface temperature, the ocean captures more heat. There is also an approximately linear relationship between the sea surface temperature and the North Atlantic MOC intensity (Fig. 12). In contrast, there is no clear change in the upper ocean heat content related with the MOC sensitivity. Therefore, the CO_2 sensitivity has a stronger effect on the ocean behaviour than MOC sensitivity. In other words, even though we selected parameter sets in a large phase space, the ocean is responding more to the atmospheric forcing than to its intrinsic characteristics. The initial states of the ocean, that are different depending on the parameter sets, do not induce large changes in the upper ocean heat content neither.

Although none of the selected parameter sets is able to provide a perfect balance that would yield climate simulation in the range of observations for all the variables examined, some parameter sets are performing better. The purpose of the next section is to identify the parameter sets that lead to the best simulation of the climate trend over the last century.

CPD
6, 711–765, 2010

7 Performance of the parameter sets: design of a metric

In this section, we focus on the design of a metric that quantifies the ability of a simulation (i.e. a given parameter set and a given configuration) to simulate the observed climate change over the last century. This metric is a measure of the adequacy between the simulated and observationally-based trends of several climatic indicators during the 20th century. Indeed, as long as we are interested in climate change, it is more important to simulate a correct evolution of the variables, which is depending on climate sensitivity, rather than a correct value at some time, which does not presume good simulation of climate change. Specifically, the selected variables are, as in Sect. 6, the global annual mean surface temperature, atmospheric CO_2 concentration, minimum sea ice extent in the Northern Hemisphere and ocean heat content of the upper 700 m of the global ocean. Some of the data used and the principle of analysis are similar to Sect. 6, but with a much more quantitative goal here. For completeness and an easier reference, the full procedure is thus explained in detail below. Trends are computed over several decades of the last century according to the length of the dataset available for comparison (Table 5). For model results, trend is defined here as the slope of the straight line fitted by linear regression through the mean of the five members of an ensemble corresponding to the same parameter set and the same configuration. Table 5 summarises for each variable the considered time interval and the reference for the observational dataset. Similarly, the trend in the data is computed as the slope of the straight line fitted by linear regression through this dataset. Two datasets for minimum sea ice extent and ocean heat content are used for the metric. It should be noted that, for the most part, the sea ice extent data rely on the same observations. The end product only differs in the analysis systems and methodology used.

For given a variable (b_i) and corresponding reference (b_{obs}), we define the ratio (R_i) of their difference to the median (M) of the deviation from observations for all the simulations (i.e. all the parameter sets) of a given setup (either Conc or Efor).

CPD
6, 711–765, 2010
Climate model performance over the last centuries
M. F. Loutre et al.

Actually, M is the median of $\mathrm{abs}(b_i - b_{\mathrm{obs}})$. Following Gleckler et al. (2008), we define a "typical" error as the median rather than the mean value to reduce the weight of outliers (simulations with unusually large error). The metric is thus defined as follows:

$$R_i = \frac{\mathrm{abs}(b_i - b_{\mathrm{obs}})}{M}$$

The index i stands for each of the 54 experiments with combinations of the nine climate parameter sets, the three carbon parameter sets, and both S1 and S2 sulphate forcings. The procedure is conducted separately for the Conc and Efor setups. The value of R yields a measure of how well a given set of parameters (i), with a given experimental setup, compares with a typical simulation. For example, if R_i equals one, then the difference between the simulation (mean over five members) and the observations is the same as the median error for all simulations. If $R_i < 1$ ($R_i > 1$), the simulation performs better (worse) than the median. If the trend in the simulation and in the observations is the same, R_i is zero.

The performance of each simulation for each variable is assessed with a threshold value for R_i, set here to 0.66. One point is attributed to a particular parameter set and configuration if R_i is less than 0.66 and no point otherwise. One point is attributed for the ocean heat content or the sea ice extent if the simulation performs well with respect to at least one of the observational datasets. The total score (the metric) is computed as the total number of good performances for each variable. None of the simulations received the maximum score of four (Conc) or six (Efor) points. The best simulations received a total score of three (Conc) and four (Efor) points (Fig. 13).

It appears that no simulation is perfect. In particular, none can simulate simultaneously a correct time evolution for the Northern Hemisphere sea ice extent and for the ocean heat content in the upper 700 m. Simulations with the carbon parameter set 3 do not properly reproduce the observed atmospheric CO_2 increase. Still it must be underlined that the deviation from observations remains less than 10 ppmv over the last 50 years. Moreover, this does not prevent to simulate a temperature increase in agreement with observations.

The aerosol forcing scenario (S1 or S2) has a strong impact on the skill of a parameter set to reproduce the climate change for a given variable. For example, more parameter sets perform well in reproducing the ocean heat content trend under S2 than S1 aerosol forcing. On the contrary, the temperature increase over the 20th century and of the last decades is better simulated with S1 than S2 sulphate forcing.

When atmospheric CO_2 concentration is prescribed (Conc), most of the parameter sets, except those with the lowest CO_2 sensitivity, are able to reproduce the temperature trend over the 20th century. The trend in upper ocean heat content remains within the selected range for the low CO_2 sensitivity parameter sets. A few more parameter sets lead to acceptable range when S2 aerosol forcing is used.

Generally speaking, simulations with high climate sensitivity (32, 41, 51, 52) have a better global score than simulations with low CO_2 sensitivity. Amongst the simulations ranking the highest (i.e. a final mark of three for Conc and four for Efor), configuration 321 is the only one performing well for both Conc and Efor, as well as for S1 and S2 sulphate aerosol forcings. Moreover, other configurations (322, 511, 512) display good performance for both Conc and Efor, either for S1 or S2 sulphate aerosol forcing.

The 321-parameter set is performing particularly well. Its major weakness is the simulation of the evolution of the upper ocean heat content in the case of S1 sulphate forcing and long-term temperature (and CO_2) in case of S2 sulphate aerosol forcing. Simulating an increase of the upper ocean heat content in line with observation is also a major problem for the other "good" parameter sets (except for 322 under Conc-configuration with S2 sulphate aerosol forcing).

The difficulty of simulating properly the increase in the upper ocean heat content is a rather general feature of all the simulations, especially those with high CO_2 sensitivity. The parameter sets identified as having a "good skill" to reproduce the 20th century climate trend are those allowing a good simulation of the atmospheric temperature increase of the last century and the last decades of that century. However, their skill in reproducing the increase in the upper ocean heat content is much poorer. Conversely, the parameter sets leading to a good representation of the trend in upper ocean heat

CPD
6, 711–765, 2010

content lead to a too weak global warming over the last century and last decades.

The heat uptake by the ocean is probably too large to allow for a good representation of both atmospheric temperature and ocean heat content. Moreover, Fig. 11 shows a linear relationship between the increase in sea surface temperature and the increase in ocean heat uptake. We speculate that a too large ocean heat uptake leads to a deficit in energy available at the ocean surface for melting the sea ice simulated with several parameter sets.

Using the S2 sulphate forcing does not significantly improve this situation. Still some parameter sets with a CO_2 sensitivity of 2.5 to 3 °C are able to simulate acceptable increase in global annual surface temperature and upper ocean heat content, although this balance is reached with a too low temperature increase and a too high upper ocean heat content. At this stage, we should also remind the reader that the skill of the parameter sets is computed on a small set of variables. Therefore, another set of variables, for example giving more weight to the ocean component of the system, could give rise to a slightly different conclusion about the skill of the parameter sets.

It is worth mentioning that most of the parameter sets selected as having a good skill simulate temperature increase over the last decades in line with the observations, although the temperature change over the whole century is slightly less well reproduced. On the other hand, as already underlined, most of them do not accurately capture the CO_2 trend over the last decades, although the deviation is small. Moreover, Efor experiments have two additional degrees of freedom compared to Conc, i.e. CO_2 and carbon emissions from deforestation are prognostic in the case Efor. This may explain the change in performance between Conc and Efor experiments for the same climatic parameter set. A weaker (stronger) CO_2 generates a low (high) carbon emission due to deforestation since the emission is calculated on the basis of the potential growth of trees, which is higher for higher CO_2 and/or carbon parameter sets 1 or 2. It should also be noted that the forcing conditions related to the carbon cycle are depending on the climate parameter set.

CPD
6, 711–765, 2010

The raw R-values can take rather large values, meaning a strong discrepancy between the simulated and observed trends. This is even true for parameter sets that exhibit a good overall skill. For example, the 321-parameter set (under Conc-setup) yields large R-values for the upper ocean heat content with S1 sulphate aerosol forcing. Conversely, some parameter sets, which yield a low skill, actually display too large individual R-values. The mean R-value of 211 for all the variables is less than 1 under Conc-setup; however, it is lower than the selected threshold for only one variable and larger than one for several of them. This also highlights how critical the choice of the threshold value is which separates between "good" and "poor" agreement.

8 Conclusions

In this paper, we selected 27 parameter sets (nine climate parameters and three carbon parameters) and we assessed their ability (1) to cover a large range of potential climate behaviours over the next millennium, (2) to simulate properly the major features of the present-day climate, and (3) to simulate reasonably well the climate changes over the last millennium.

This work is part of a study that aims to study uncertainties in modelling experiments used in climate change projections. Different approaches could be used. For example, using various models or different external forcings often yields a wide range of responses. Here, we used different values for the selected parameter sets. The associated uncertainties in climate, characterised through global annual mean surface temperature, atmospheric CO_2 concentration, minimum Northern Hemisphere sea ice extent and upper ocean heat content, are quantified through transient experiments over the last millennium. We designed a metric in order to quantify the skill of the different parameter sets to reproduce the climate change over the last decades of the 20th century.

This is clearly a step forward compared to studies using only one parameter set. Nevertheless, by using one single model, we did not address the structural uncertainty that can also be a major source of discrepancy between model results. Ideally, both types of uncertainties should be addressed together, in addition to the ones associated with the forcing, but this long-term goal is clearly outside the scope of the present study.

We used our expert judgment to select a small and manageable number of parameter sets. Obviously, others could also have been chosen, but these were selected because we knew their individual effect on the modelled climate and we knew for sure that they would yield a range of different model behaviours, according to the model sensitivity to an increase in atmospheric CO_2 concentration, to its response to a freshwater hosing and to its sensitivity to carbon cycle. However, their combined effect is strongly dominated by the model sensitivity to an increase in atmospheric CO_2 concentration. Indeed, the mean ocean state or the model response to a freshwater hosing has almost no impact even on the ocean behaviour over the last century. Moreover, we showed that very few parameter sets are able to reproduce the observed trend of some key variables of the climate system (e.g. surface temperature, atmospheric CO_2 concentration, sea ice extent, ocean heat content). Therefore, we can use this work to reduce the number of parameter sets, keeping only the best in simulating climate with LOVECLIM. Alternatively, we can keep them all to cover a wide range of possible climates although it must then be kept in mind that some yield a less realistic behaviour, at least for some components of the climate system. This second alternative allows coverage of more extreme cases that must be assessed in the light of the simulation of past climate. For example, less weight could then be given to a simulation performed with a low skill parameter set.

Varying the value of key physical parameters of LOVECLIM cannot solve clearly identified drawbacks as underlined by some systematic biases present with all the parameter sets. In other words, further tuning will most probably be relatively ineffective to improve the model behaviour to simulate past climates, at least for some variables and in some regions. Still, EMICs remain very useful to cover a wide range of climate states. On the contrary, GCMs aims at simulating as accurately as possible the "true" climate. Therefore, both GCMs and EMICs should be used complementarily to better constrain uncertainties in climate projections.

CPD
6, 711–765, 2010

Acknowledgements. This study was funded by the Belgian Federal Science Policy within its Research Programme on Science for a Sustainable Development (SD/CS/01). We thank Pierre-Yves Barriat for helping in developments of the computer code. H. Goosse is Research Associate with the Fonds National de la Recherche Scientifique (Belgium). Computer time was partly made available by UCL (Fonds spéciaux de recherche) and FNRS (Fonds de la recherche fondamentale collective) FRFC No. 2.4502.05: "Simulation numérique. Application en physique de l'état solide, océanographie et dynamique des fluides". We also thank the CISM-team.

References

Barnola, J.-M., Anklin, M., Porcheron, J., Raynaud, D., Schwander, J., and Stauffer, B.: CO_2 evolution during the last millennium as recorded from Antarctica and Greenland ice, Tellus B, 47, 264–272, 1995.

Berger, A.: Long-term variations of daily insolation and Quaternary climatic changes, J. Atmos. Sci., 35(12), 2362–2367, 1978.

Berger, W. H., Fischer, K., Lai, C., and Wu, G.: Ocean Productivity and Organic Carbon Flux. Part I. Overview and Maps of Primary Production and Export Production, SIO (University of California, Scripps Institution of Oceanography), Reference Series 87–30, 66 pp., 1987.

Bertrand, C., Loutre, M. F., Crucifix, M., and Berger, A.: Climate of the last millennium: a sensitivity study, Tellus A, 54, 221–244, 2002.

Betzer, P. R., Byrne, R. H., Acker, J. G., Lewis, C. S., and Jolley, R. R.: The oceanic carbonate system: a reassessment of biogenic controls, Science, 226, 1074–1077, 1984.

Braconnot, P., Loutre, M. F., Dong, B., Joussaume, S., and Valdes, P.: (2002). How the simulated change in monsoon at 6 ka BP is related to the simulation of the modern climate: results from the Paleoclimate Modeling Intercomparison Project, Clim. Dynam., 19, 107–121, 2002.

Braconnot, P., Otto-Bliesner, B., Harrison, S., Joussaume, S., Peterchmitt, J.-Y., Abe-Ouchi, A., Crucifix, M., Driesschaert, E., Fichefet, Th., Hewitt, C. D., Kageyama, M., Kitoh, A., Laîné, A., Loutre, M.-F., Marti, O., Merkel, U., Ramstein, G., Valdes, P., Weber, S. L., Yu, Y., and Zhao, Y.: Results of PMIP2 coupled simulations of the Mid-Holocene and Last Glacial Maximum – Part 1: experiments and large-scale features, Clim. Past, 3, 261–277, 2007a, http://www.clim-past.net/3/261/2007/.

Braconnot, P., Otto-Bliesner, B., Harrison, S., Joussaume, S., Peterchmitt, J.-Y., Abe-Ouchi, A., Crucifix, M., Driesschaert, E., Fichefet, Th., Hewitt, C. D., Kageyama, M., Kitoh, A., Loutre, M.-F., Marti, O., Merkel, U., Ramstein, G., Valdes, P., Weber, L., Yu, Y., and Zhao, Y.: Results of PMIP2 coupled simulations of the Mid-Holocene and Last Glacial Maximum Part 2: feedbacks with emphasis on the location of the ITCZ and mid- and high latitudes heat budget, Clim. Past, 3, 279–296, 2007b, http://www.clim-past.net/3/279/2007/.

Bretagnon, P.: Théorie du mouvement de l'ensemble des planètes. Solution VSOP82, Astron. Astrophys., 30, 141–154, 1982 (in French).

Brierley, C. M., Collins, M., and Thorpe, A. J.: The impact of perturbations to ocean-model parameters on climate and climate change in a coupled model, Clim. Dynam., 34, 325–343, doi:10.1007/s00382-008-0486-3, 2010.

Briffa, K. R.: Annual climate variability in the Holocene: interpreting the message of ancient trees, Quaternary Sci. Rev., 19(1–5), 87–105, 2000.

Briffa, K. R., Osborn, T., Schweingruber, F., Harris, I., Jones, P., Shiyatov, S., and Vaganov, E.: Low-frequency temperature variations from a northern tree ring density network, J. Geophys. Res., 106(D3), 2929–2941, 2001.

Briffa, K. R., Osborn, T. J., and Schweingruber, F. H.: Large-scale temperature inferences from tree rings: a review, Global Planet. Change, 40(1–2), 11–26, 2004.

Brohan, P, Kennedy, J. J., Harris, I., Tett, S. F. B., and Jones, P. D.: Uncertainty estimates in regional and global observed temperature changes: a new dataset from 1850, J. Geophys. Res., 11(D12), D12106, doi:10.1029/2005JD006548, 2006.

Brovkin, V., Bendsten, J., Claussen, M., Ganopolski, A., Kubatzki, C., Petoukhov, V., and Andreev, A.: Carbon cycle, vegetation and climate dynamics in the Holocene: Experiment with the CLIMBER-2 model, Global Biogeochem. Cy., 16(4), 1139, doi:10.1029/2001GB001662, 2002.

Brovkin, V., Claussen, M., Driesschaert, E., Fichefet, T., Kicklighter, D., Loutre, M. F., Matthews, H. D., Ramankutty, N., Schaeffer, M., and Sokolov, A.: Biogeophysical effects of historical land cover changes simulated by six Earth system models of intermediate complexity, Clim. Dynam., 26(6), 587–600, doi:10.1007/s00382-005-0092-6, 2006.

Bryan, K. and Lewis, L. J.: A water mass model of the world ocean, J. Geophys. Res., 84(C5), 2503–2517, 1979.

Charlson, R., Langmer, J., Rodhe, H., Levoy, C., and Warren, S.: Perturbation of the Northern hemisphere radiative balance by backscattering from anthropogenic sulfate aerosols, Tellus AB, 43, 152–163, 1991.

Chou, C. and Neelin, J. D.: Linearization of a long-wave radiation scheme for intermediate tropical atmospheric model, J. Geophys. Res., 101(D10), 15129–15145, 1996.

Collins, M., Brierley, C. M., MacVean, M., Booth, B. B. B., and Harris, G. R.: The sensitivity of the rate of transient climate change to ocean physics perturbations, J. Climate, 20(10), 2315–2320, doi:10.1175/ JCLI4116.1, 2007.

Comiso, J. C. and Nishio, F.: Trends in the Sea Ice Cover Using Enhanced and Compatible AMSR-E, SSM/I, and SMMR Data. J. Geophys. Res., 113, C02S07, doi:10.1029/2007JC004257, 2008.

Cook, E. R., Esper, J., and D'Arrigo, R. D.: Extra-tropical Northern Hemisphere land temperature variability over the past 1000 years, Quaternary Sci. Rev., 23(20–22), 2063–2074, 2004.

Crowley, T.: Causes of climate change over the past 1000 years, Science, 289, 270–277, 2000.

D'Arrigo, R., Wilson, R., and Jacoby, G.: On the long-term context for late twentieth century warming, J. Geophys. Res., 111, D03103, doi:10.1029/2005JD006352, 2006.

Dixon, K. and Lanzante, J.: Global mean surface air temperature and North Atlantic overturning in a suite of coupled GCM climate change experiments, Geophys. Res. Lett., 26, 1885–1888, 1999.

Domingues, C. M., Church, J. A., White, N. J., Gleckler, P. J., Wijffels, S. E., Barker, P. M., and Dunn, J. R.: Improved estimates of upper-ocean warming and multi-decadal sea-level rise, Nature, 453, 1090–1093, doi:10.1038/nature07080, 2008.

Driesschaert, E., Fichefet, T., Goosse, H., Huybrechts, P., Janssens, I., Mouchet, A., Munhoven, G., Brovkin, V., and Weber, S. L.: Modeling the influence of Greenland ice sheet melting on the meridional overturning circulation during the next millennia, Geophys. Res. Lett., 34, L10707, doi:10.1029/2007GL029516, 2007.

Dutay, J.-C., Jean-Baptiste, P., Campin, J.-M., Ishida, A., Maier-Reimer, E., Matear, R. J., Mouchet, A., Totterdell, I. J., Yamanaka, Y., Rodgers, K., Madec, G., and Orr, J. C.: Evaluation of OCMIP-2 ocean models' deep circulation with mantle helium-3, J. Marine Syst., 48, 15–36, doi:10.1016/j.jmarsys.2003.05.010, 2004.

Enting, I. G., Wigley, T. M. L., and Heimann, M.: Future Emissions and Concentrations of Carbon Dioxide: Key Ocean/Atmosphere/Land Analyses, CSIRO Aust. Div. Atmos. Res.,

Tech. Pap., 31, 1–118, 1994.
Esper, J., Cook, E. R., and Schweingruber, F. H.: Low-frequency signals in long tree-ring chronologies for reconvariability, Science, 295(5563), 2250–2253, 2002.
Etheridge, D. M., Steele, L. P., Langenfelds, R. L., Francey, R. J., Barnola, J.-M., and Morgan, V. I.: Historical CO_2 records from the Law Dome DE08, DE08-2, and DSS ice cores, in: Trends: A Compendium of Data on Global Change, Carbon Dioxide Information Analysis Center, Oak Ridge National Laboratory, US Department of Energy, Oak Ridge, TN, USA, 1998.
Flückiger, J., Monnin, E., Stauffer, B., Schwander, J., Stocker, T.F., Chappellaz, J., Raynaud, D., and Barnola, J.M.: High-resolution Holocene N_2O ice core record and its relationship with CH_4 and CO_2, Global Biogeochem. Cy., 16, 1, doi:10.1029/2001GB001417, 2002.
Forster, P., Ramaswamy, V., Artaxo, P., Berntsen, T., Betts, R., Fahey, D. W., Haywood, J., Lean, J., Lowe, D. C., Myhre, G., Nganga, J., Prinn, R., Raga, G., Schulz, M., and Van Dorland, R.: Changes in Atmospheric Constituents and in Radiative Forcing, in: Climate Change 2007: The Physical Science Basis. Contribution of Working Group I to the Fourth Assessment Report of the Intergovernmental Panel on Climate Change, edited by: Solomon, S., Qin, D., Manning, M., Chen, Z., Marquis, M., Averyt, K. B., Tignor, M., and Miller, H. L., Cambridge University Press, Cambridge, United Kingdom and New York, NY, USA, 2007.
Frank, D. C, Esper, J., Raible, C. C., Büntgen, U., Trouet, V., Stocker, B., and Joos, F.: Ensemble reconstruction constraints on the global carbon cycle sensitivity to climate, Nature, 463, 527–532, doi:10.1038/nature08769, 2010.
Friedlingstein, P., Dufresne, J.-L., Cox, P. M., and Rayner, P.: How positive is the feedback between climate change and the carbon cycle?, Tellus B, 55, 692–700, 2003.
Gent, P.: Will the North Atlantic Ocean thermohaline circulation weaken during the 21st century?, Geophys. Res. Lett., 28, 1023–1026, 2001.
Gleckler, P. J., Taylor, K. E., and Doutriaux, C.: Performance metrics for climate models. J. Geophys. Res., 113(D6), D06104, doi:10.1029/2007JD008972, 2008.
GLOBALVIEW-CO2: Cooperative Atmospheric Data Integration Project - Carbon Dioxide. CD-ROM, NOAA GMD, Boulder, Colorado, also available on Internet via anonymous FTP to ftp.cmdl.noaa.gov, Path: ccg/co2/GLOBALVIEW, 2006.
Goelzer, H., Huybrechts, P., Loutre, M. F., Goosse, H., Fichefet, T., and Mouchet, A.: Impact of Greenland and Antarctic ice sheet interactions on climate sensitivity, Clim. Dynam., submitted, 2010.

Goosse, H. and Fichefet, H.: Importance of ice-ocean interactions for the global ocean circulation : A model study, J. Geophys. Res., 104, 23337–23355, 1999.
Goosse, H., Deleersnijder, E., Fichefet, T., and England, M. H.: Sensitivity of a global coupled ocean-sea ice model to the parameterization of vertical mixing, J. Geophys. Res., 104(C6), 13681–13695, 1999.
Goosse, H., Selten, F. M., Haarsma, R. J., and Opsteegh, J. D.: Decadal variability in high northern latitudes as simulated by an intermediate complexity climate model, Ann. Glaciol., 33, 525–532, 2001.
Goosse, H., Crowley, T., Zorita, E., Ammann, C., Renssen, H., and Driesschaert, E.: Modelling the climate of the last millennium: What causes the differences between simulations?, Geophys. Res. Lett., 32, L06710, doi:10.1029/2005GL22368, 2005.
Goosse, H., Driesschaert, E., Fichefet, T., and Loutre, M.-F.: Information on the early Holocene climate constrains the summer sea ice projections for the 21st century, Clim. Past, 3, 683–692, 2007, http://www.clim-past.net/3/683/2007/.
Goosse, H., Brovkin, V., Fichefet, T., Haarsma, R., Huybrechts, P., Jongma, J., Mouchet, A., Selten, F., Barriat, P.-Y., Campin, J.-M., Deleersnijder, E., Driesschaert, E., Goelzer, H., Janssens, I., Loutre, M.-F., Morales Maqueda, M. A., Opsteegh, T., Mathieu, P.-P., Munhoven, G., Pettersson, E. J., Renssen, H., Roche, D. M., Schaeffer, M., Tartinville, B., Timmermann, A., and Weber, S. L.: Description of the Earth system model of intermediate complexity LOVECLIM version 1.2, Geosci. Model Dev. Discuss., 3, 309–390, 2010.
Gregory, J. M., Dixon, K. W., Stouffer, R. J., Weaver, A. J., Driesschaert, E., Eby, M., Fichefet, T., Hasumi, H., Hu, A., Jungclaus, J. H., Kamenkovich, I. V., Levermann, A., Montoya, M., Murakami, S., Nawrath, S., Oka, A., Sokolov, A. P., and Thorpe, R. B.: A model intercomparison of changes in the Atlantic thermohaline circulation in response to increasing atmospheric CO_2 concentration, Geophys. Res. Lett., 32, L12703, doi:10.1029/2005GL023209, 2005.
Haarsma, R. J., Selten, F. M., Opsteegh, J. D., Lenderink, G., and Liu, Q.: ECBILT, a coupled atmosphere ocean sea-ice model for climate predictability studies, KNMI, De Bilt, The Netherlands, 31 pp., 1996.
Hegerl, G. C., Crowley, T. J., Hyde, W. T., and Frame, D. J.: Climate sensitivity constrained by temperature reconstructions over the past seven centuries, Nature, 440, 1029–1032, 2006.
Houghton, R. A.: Revised estimates of the annual net flux of carbon to the atmosphere from changes in land use and land management 1850–2000, Tellus B, 55(2), 378–390, 2003.

Houghton, J. T., Jenkins, G. J., and Ephraums, J. J. (Eds.): Climate Change: The IPCC Scientific Assessment, Cambridge University Press, Cambridge, 365 pp., 1990.
Houghton, J. T., Ding, Y., Griggs, D. J., Noguer, M., van der Linden, P. J., Dai, X., Maskell, K., and Johnson, C. A.: Climate Change 2001: The Scientific Basis, in: Contribution of Working Group I to the Third Assessment Report of the Intergovernmental Panel on Climate Change, Cambridge University Press, 881 pp., 2001.
Huybrechts, P.: A 3-D model for the Antarctic ice sheet: a sensitivity study on the glacial-interglacial contrast, Clim. Dynam., 5, 79–92, 1990.
Huybrechts, P.: Basal temperature conditions of the Greenland ice sheet during the glacial cycles, Ann. Glaciol., 23, 226–236, 1996.
Huybrechts, P. and de Wolde J.: The dynamic response of the Greenland and Antarctic ice sheets to multiple-century climatic warming, J. Climate, 12, 2169–2188, 1999.
Indermühle, A., Stocker, T. F., Joos, F., Fischer, H., Smith, H. J., Wahlen, M., Deck, B., Mastroianni, D., Tschumi, J., Blunier, T., Meyer, R., and Stauffer, B.: Holocene carbon-cycle dynamics based on CO_2 trapped in ice at Taylor Dome, Antarctica, Nature, 398, 121–126, 1999.
IPCC: Climate Change 2007: The Physical Science Basis, in: Contribution of Working Group I to the Fourth Assessment Report of the Intergovernmental Panel on Climate Change, edited by: Solomon, S., Qin, D., Manning, M., Chen, Z., Marquis, M., Averyt, K. B., Tignor, M., and Miller, H. L., Cambridge University Press, Cambridge, United Kingdom and New York, NY, USA, 996 pp., 2007.
Jansen, E., Overpeck, J., Briffa, K. R., Duplessy, J.-C., Joos, F., Masson-Delmotte, V., Olago, D., Otto-Bliesner, B., Peltier, W. R., Rahmstorf, S., Ramesh, R., Raynaud, D., Rind, D., Solomina, O., Villalba R., and Zhang, D.: Palaeoclimate, in: Climate Change 2007: The Physical Science Basis. Contribution of Working Group I to the Fourth Assessment Report of the Intergovernmental Panel on Climate Change, edited by: Solomon, S., Qin, D., Manning, M., Chen, Z., Marquis, M., Averyt, K. B., Tignor, M., and Miller, H. L., Cambridge University Press, Cambridge, United Kingdom and New York, NY, USA, 2007.
Jones, P. D., Briffa, K. R., Barnett, T. P., and Tett, S. F. B.: High-resolution palaeoclimatic records for the last millennium: interpretation, integration and comparison with General Circulation Model control-run temperatures, The Holocene, 8(4), 455–471, 1998.
Jones, P. D., Osborn, T. J., and Briffa, K. R.: The evolution of climate over the last millennium, Science, 292(5517), 662–667, 2001.

CPD
6, 711–765, 2010

Climate model performance over the last centuries

M. F. Loutre et al.

Klaas, C. and Archer, D.: Association of sinking organic matter with various types of mineral ballast in the deep sea: Implications for the rain ratio, Global Biogeochem. Cy., 16, 1116, doi:10.1029/2001GB001765, 2002.
Knutti, R., Allen, M. R., Friedlingstein, P., Gregory, J. M., Hegerl, G. C., Meehl, G. G. A., Meinshausen, M., Murphy, J. M., Plattner, G.-K., Raper, S. C. B., Stocker, T. F., Stott, P. A., Teng, H., and Wigley, T. M. L.: A Review of Uncertainties in Global Temperature Projections over the Twenty-First Century, J. Climate, 21, 2651–2663, doi:10.1175/2007JCLI2119.1, 2008.
Levitus, S., Antonov, J. I., Boyer, T. P., Locarnini, R. A., Garcia, H. E., and Mishonov, A. V.: Global ocean heat content 1955–2008 in light of recently revealed instrumentation problems. Geophys. Res. Lett., 36, L07608, doi:10.1029/2008GL037155, 2009.
Mann, M. E., Bradley, R. S., and Hughes, M. K.: Northern hemisphere temperatures during the past millennium: Inferences, uncertainties, and limitations, Geophys. Res. Lett., 26(6), 759–762, 1999.
Mann, M. E. and Jones, P. D.: Global surface temperatures over the past two millennia, Geophys. Res. Lett., 30(15), 1820, doi:10.1029/2003GL017814, 2003.
Marland, G., Boden, T., and Andres, R.: Global, Regional, and National Annual CO_2 Emissions from Fossil-Fuel Burning, Cement Production, and Gas Flaring: 1751—2000, in: Trends: A compendium of data on global change, published by Carbon Dioxide Information Analysis Center, Oak Ridge, TN, 2003.
Martin, J. H., Knauer, G. A., Karl, D. M., and Broenkow, W. W.: VERTEX: carbon cycling in the northeast Pacific, Deep-Sea Res., 34, 267–285, 1987.
Meehl, G. A., Stocker, T. F., Collins, W. D., Friedlingstein, P., Gaye, A. T., Gregory, J. M., Kitoh, A., Knutti, R., Murphy, J. M., Noda, A., Raper, S. C. B., Watterson, I. G., Weaver, A. J., and Zhao, Z.-C.: Global Climate Projections, in: Climate Change 2007: The Physical Science Basis. Contribution of Working Group I to the Fourth Assessment Report of the Intergovernmental Panel on Climate Change, edited by: Solomon, S., Qin, D., Manning, M., Chen, Z., Marquis, M., Averyt, K. B., Tignor, M., and Miller, H. L., Cambridge University Press, Cambridge, United Kingdom and New York, NY, USA, 2007.
Menviel, L., Timmermann, A., Mouchet, A., and Timm, O.: Meridional reorganizations of marine and terrestrial productivity during Heinrich events, Paleoceanography, 23, PA1203, doi:10.1029/2007PA0014455, 2008a.
Menviel, L., Timmermann, A., Mouchet, A., and Timm, O.: Climate and marine carbon cycle response to changes in the strength of the Southern Hemispheric westerlies, Paleoceanog-

CPD
6, 711–765, 2010

Climate model performance over the last centuries

M. F. Loutre et al.

raphy, 23, PA4201, doi:10.1029/2008PA001604, 2008b.
Meure, C. M., Etheridge, D., Trudinger, C., Steele, P., Langenfelds, R., van Ommen, T., Smith, A., and Elkins, J.: Law Dome CO_2, CH_4 and N_2O ice core records extended to 2000 years BP, Geophys. Res. Lett., 3(14), L14810, doi:10.1029/2006GL026152, 2006.
Moberg, A., Sonechkin, D. M., Holmgren, K., Datsenko, N. M., and Karlén, W.: Highly variable Northern Hemisphere temperatures reconstructed from low- and high-resolution proxy data, Nature, 433(7026), 613–617, 2005.
Monnin, E., Steig, E. J., Siegenthaler, U., Kawamura, K., Schwander, J., Stauffer, B., Stocker, T. F., Morse, D. L., Barnola, J. M., Bellier, B., Raynaud, D., and Fischer, H.: (2004). Evidence for substantial accumulation rate variability in Antarctica during the Holocene, through synchronization of CO_2 in the Taylor Dome, Dome C and DML ice cores, Earth Planet. Sc. Lett., 224(1–2), 45–54, doi:10.1016/j.epsl.2004.05.007, 2004.
Mouchet, A.: A 3D model of ocean biogeochemical cycles and climate sensitivity studies, Ph.D. thesis, Université de Liège, Liège, Belgium, 2010.
Mouchet, A. and François, L. M.: Sensitivity of a global oceanic carbon cycle model to the circulation and to the fate of organic matter: preliminary results, Phys. Chem. Earth, 21, 511–516, 1996.
Murphy, J. M., Sexton, D. M. H., Barnett, D. N., Jones, G. S., Webb, M. J., Collins, M., and Stainforth, A. A.: Quantification of modelling uncertainties in a large ensemble of climate change simulations, Nature, 430, 768–772, 2004.
Muscheler, R., Joos, F., Beer, J., Muller, S. A., Vonmoos, M., and Snowball, I.: Solar activity during the last 1000 yr inferred from radionuclide records, Quaternary Sci. Rev., 26(1–2), 82–97, 2007.
Nakicenovic, N. and Swart, R. (Eds.): Special report on emissions scenarios, in: A special report of Working Group III of the Intergovernmental Panel on Climate Change, Cambridge University Press, Cambridge, United Kingdom and New York, NY, USA, 599 pp., 2000.
Neftel, A., Friedli, H., Moor, E., Lotscher, H., Oeschger, H., Siegenthaler, U., and Stauffer, B.: Historic CO_2 record from the Siple Station ice core, in: Trends '93: A Compendium of Data on Global Change. ORNL/CDIAC-65, edited by: Boden, T.A., Kaiser, D. P., Sepanski, R. J., and Stoss, F. W., Carbon Dioxide Information Analysis Center, Oak Ridge National Laboratory, Oak Ridge, TN, USA, 11–14, 1994.
Opsteegh, J. D., Haarsma, R. J., Selten, F. M., and Kattenberg, A.: ECBILT: A dynamic alternative to mixed boundary conditions in ocean models, Tellus A, 50, 348–367, 1998.

Pollack, H. N. and Smerdon, J. E.: Borehole climate reconstructions: Spatial structure and hemispheric averages, J. Geophys. Res., 109(D11), D11106, doi:10.1029/2003JD004163, 2004.

Prather, M., Ehhalt, D., Dentener, F., Derwent, R., Dlugokencky, E., Holland, E., Isaksen, I., Katima, J., Kirchhoff, V., Matson, P., Midgley, P., and Wang, M.: Atmospheric chemistry and greenhouse gases, in: Climate Change 2001: The Scientific Basis. Contribution of Working Group I to the Third Assessment Report of the Intergovernmental Panel on Climate Change, edited by: Houghton, J. T., Ding, Y., Griggs, D. J., Noguer, M., van der Linden, P. J., Dai, X., Maskell, K., and Johnson, C. A., Cambridge University Press, Cambridge, United Kingdom and New York, NY, USA, 881 pp., 2001.

Rahmstorf, S., Crucifix, M., Ganopolski, A., Goosse, H., Kamenkovich, I., Knutti, R., Lohmann, G., Marsh, B., Mysak, L., Wang, Z., and Weaver, A.: Thermohaline circulation hysteresis: a model intercomparison, Geophys. Res. Lett., 32, L23605, doi:10.1029/2005GL23655, 2005.

Ramankutty, N. and Foley, J. A.: Estimating historical changes in global land cover : Croplands from 1700 to 1992, Global Biogeochem. Cy., 13(4), 997–1027, 1999.

Randall, D. A., Wood, R. A., Bony, S., Colman, R., Fichefet, T., Fyfe, J., Kattsov, V., Pitman, A., Shukla, J., Srinivasan, J., Stouffer, R. J., Sumi, A., and Taylor, K. E.: Cilmate Models and Their Evaluation, in: Climate Change 2007: The Physical Science Basis. Contribution of Working Group I to the Fourth Assessment Report of the Intergovernmental Panel on Climate Change, edited by: Solomon, S., Qin, D., Manning, M., Chen, Z., Marquis, M., Averyt, K. B., Tignor, M., and Miller, H. L., Cambridge University Press, Cambridge, United Kingdom and New York, NY, USA, 2007.

Renssen, H., Goosse, H., and Fichefet, T.: Modeling the effect of freshwater pulses on the early Holocene climate: The influence of high-frequency climate variability, Paleoceanography, 17(2), 1020, doi:10.1029/2001PA000649, 2002.

Rutherford, S., Mann, M. E., Osborn, T. J., Bradley, R. S., Briffa, K. R., Hughes, M. K., and Jones, P. D.: Proxy-based Northern Hemisphere surface temperature reconstructions: Sensitivity to method, predictor network, target season, and target domain, J. Climate, 18(13), 2308–2329, 2005.

Schaeffer, M., Selten, F., and van Dorland, R.: Linking Image and ECBILT. National Institute for public health and the environment (RIVM), Bilthoven, The Netherlands, Report no 4815008008, 1998.

CPD

6, 711–765, 2010

Climate model performance over the last centuries

M. F. Loutre et al.

Shine, K. P. and Henderson-Sellers, A.: The sensitivity of a thermodynamic sea ice model to changes in surface albedo parameterization, J. Geophys. Res., 90(D1), 2243-2250, doi:10.1029/JD090iD01p02243, 1985.

Siegenthaler, U., Monnin, E., Kawamura, K., Spahni, R., Schwander, J., Stauffer, B., Stocker, T. F., Barnola, J.-M., and Fischer, H.: Supporting evidence from the EPICA Dronning Maud Land ice core for atmospheric CO_2 changes during the past millennium, Tellus B, 57, 51–57(7), doi:10.1111/j.1600-0889.2005.00131.x, 2005.

Stainforth, D. A., Aina, T., Christensen, C., Collins, M., Faull, N., Frame, D. J., Kettleborough, J. A., Knight, S., Martin, A., Murphy, J. M., Piani, C., Sexton, D., Smith, L. A., Spicer, R. A., Thorpe, A. J., and Allen, M. R.: Uncertainty in predictions of the climate response to rising levels of greenhouse gases, Nature, 433, 403–406, doi:10.1038/nature03301, 2005.

Stainforth, D. A., Allen, M. R., Tredger, E. R., and Smith, L. A.: Confidence, uncertainty and decision-support relevance in climate predictions, Philos. T. Roy. Soc. A, 365, 2145–2161, 2007.

Suess, E.: Particulate organic carbon flux in the ocean – surface productivity and oxygen utilization, Nature, 288, 260–263, 1980.

Weber, S. L., Drijfhout, S. S., Abe-Ouchi, A., Crucifix, M., Eby, M., Ganopolski, A., Murakami, S., Otto-Bliesner, B., and Peltier, W. R.: The modern and glacial overturning circulation in the Atlantic ocean in PMIP coupled model simulations, Clim. Past, 3, 51–64, 2007, http://www.clim-past.net/3/51/2007/.

Xie, P. P. and Arkin, P. A.: Analyses of global monthly precipitation using gauge observations, satellite estimates, and numerical model predictions, J. Climate, 9(4), 840–858, 1996.

Xie, P. P. and Arkin P. A.: Global Precipitation: A 17-year monthly analysis based on gauge observations, satellite estimates, and numerical model outputs, B. Am. Meteorol. Soc., 78(1), 2539–2558, 1997.

CPD

6, 711–765, 2010

Climate model performance over the last centuries

M. F. Loutre et al.

Table 1. The nine climatic parameter sets. The experiment names (column 1) are explained in Sect. 4. Parameters $\lambda 2$ and $\lambda 4$ (columns 2 and 3) are applied in the Rayleigh damping term of the equation of the quasi-geostrophic potential vorticity. The coefficients amplw and explw (columns 4 and 5) are used in the longwave radiative scheme to compute anomaly in humidity (see text). The uncertainties in the albedo of the ocean and sea ice are accounted for through albcoef (column 6) and albice (column 7). The minimum vertical diffusion coefficient in the ocean is scaled according to avkb (column 8). CorA is a correction factor for the distribution of precipitation over the ocean (column 9).

Name	$\lambda 2$ (m)	$\lambda 4$ (m)	amplw	explw	albocef	albice	avkb	CorA
E11	0.125	0.070	1.00	0.3333	1.000	0	1.0	–0.0850
E21	0.125	0.070	1.00	0.4	0.900	0	1.5	–0.0850
E31	0.131	0.071	1.00	0.5	0.950	0	2.5	–0,0850
E41	0.131	0.071	1.10	0.5	0.900	0	2.5	–0.0850
E51	0.131	0.071	1.30	0.5	1.050	0.02	2.0	–0.0850
E12	0.120	0.067	1.00	0.4	0.900	0	2.0	0.0000
E22	0.125	0.070	1.00	0.4	0.900	0	1.5	–0.0425
E32	0.125	0.070	1.05	0.5	0.900	0	1.5	–0.0425
E52	0.125	0.070	1.30	0.5	1.000	0.02	1.5	–0.0425

CPD
6, 711–765, 2010

Table 2. Model parameter sets for the carbon cycle and their effect on the CO_2 response. These parameters influence the continental vegetation fertilization effect (βg and βt; columns 2 and 3), the vertical flux of POM (α_{diatom} and α_{others}, columns 4 and 5), and the buildup of calcium carbonate shells (Ψ_{zoo}, column 6). Columns 7 and 8 give the maximum value of the annual mean atmospheric CO_2 concentration and its value at year 2500 from the transient simulations (see text) with the three carbon parameter sets. Climatic parameter set 11 is used here.

Carbon parameter set	βg	βt	α_{diatom}	α_{others}	Ψ_{zoo}	Atm. CO_2 (ppmv)	
						Max	2500 AD
1	0.14	0.50	–0.750	–0.950	0.10	1146	877
2	0.36	0.36	–0.858	–0.858	0.22	1202	918
3	0.14	0.22	–0.648	–0.648	0.22	1315	1010

CPD
6, 711–765, 2010

Climate model performance over the last centuries

M. F. Loutre et al.

Table 3. Main features of the model climatic parameter sets with carbon parameter set 2.

Name	CO_2 sensitivity (1)	MOC sensitivity (2)	Equilibrium MOC (3)	Ts (4)	Sea ice extent (5)		T. ocean (6)
					min.	max.	
	°C	%	Sv	°C	10^6 km^2	10^6 km^2	°C
E11	1.7	–16	28.2	16.3	9.3	14.7	3.3
E21	2.1	–29	25.9	16.0	8.7	15.1	3.0
E31	2.7	–20	25.2	16.4	8.0	14.6	3.4
E41	3.3	–25	24.7	16.0	8.0	14.8	3.2
E51	4.0	–34	23.5	16.4	7.4	14.8	3.2
E12	1.8	–52	17.5	16.1	8.4	14.3	3.1
E22	2.1	–57	23.3	15.8	8.9	15.1	2.7
E32	2.7	–54	20.5	16.0	7.4	14.8	2.7
E52	3.6	–51	20.0	16.3	6.7	14.5	2.7

(1) Increase in global annual mean surface temperature after 1000 years in the doubling CO_2 experiment from the equilibrium value;
(2) percentage of decrease in the meridional overturning streamfunction after 1000 years in the water hosing experiment;
(3) strength of the meridional overturning streamfunction in the North Atlantic (Sv) at equilibrium in the pre-industrial experiment;
(4) annual mean global surface temperature (°C) at equilibrium in the pre-industrial experiment;
(5) minimum (min) and maximum (max) of sea ice extent in the Northern Hemisphere (10^6 km^2) at equilibrium in the pre-industrial experiment;
(6) globally averaged, annual mean temperature of the ocean (°C) at equilibrium in the pre-industrial experiment.

Table 4. References for the atmospheric CO_2 concentration (top) and temperature reconstructions (bottom) presented in Fig. 7.

Series	References
CO_2 data	
Taylor Dome	Indermühle et al. (1999)
Law Dome	Etheridge et al. (1998)
Siple	Neftel et al. (1994)
South Pole	Siegenthaler et al. (2005)
D47	Barnola et al. (1995)
D57	Barnola et al. (1995)
DML	Siegenthaler et al. (2005)
Temperature reconstructions	
B2000	Briffa (2000); calibrated by Briffa et al. (2004)
BOS2001	Briffa et al. (2001)
DWJ2006	D'Arrigo et al. (2006)
ECS2002	Esper et al. (2002); recalibrated by Cook et al. (2004)
HCA2006	Hergel et al. (2006)
JBB1998	Jones et al. (1998); calibrated by Jones et al. (2001)
MBH1999	Mann et al. (1999)
MJ2003	Mann and Jones (2003)
MSH2005	Moberg et al. (2005)
PS2004	Pollack and Smerdon (2004); reference level adjusted following Moberg et al. (2005)
RMO2005	Rutherford et al. (2005)

Table 5. Column 2 gives the references of the different datasets used for comparison of the simulated time evolution for the variables given in column 1. The trend of the observations (column 4) is computed over the time interval given in column 3. cy stands for century.

Variable	Reference		
Global annual mean surface temperature	Brohan et al. (2006)	1901–2005	0.71 °C/cy
Global annual mean surface temperature	Brohan et al. (2006)	1979–2005	1.68 °C/cy
Atmospheric CO_2 concentration	Enting et al. (1994), GLOBALVIEW-CO2 (2006)	1901–2005	70 ppmv/cy
Atmospheric CO_2 concentration	Enting et al. (1994), GLOBALVIEW-CO2 (2006)	1979–2005	162 ppmv/cy
Sea ice extent	Bootstrap algorithm; Comiso and Nishio (2008)	1979–2006	-5.63×10^6 km^2/cy
Sea ice extent	Nasateam algorithm; Comiso and Nishio (2008)	1979–2007	-6.52×10^6 km^2/cy
Ocean heat content (upper 700 m)	Levitus et al. (2009)	1955–2007	26×10^{22} J/cy
Ocean heat content (upper 700 m)	Domingues et al. (2008)	1950–2003	24×10^{22} J/cy

CPD
6, 711–765, 2010

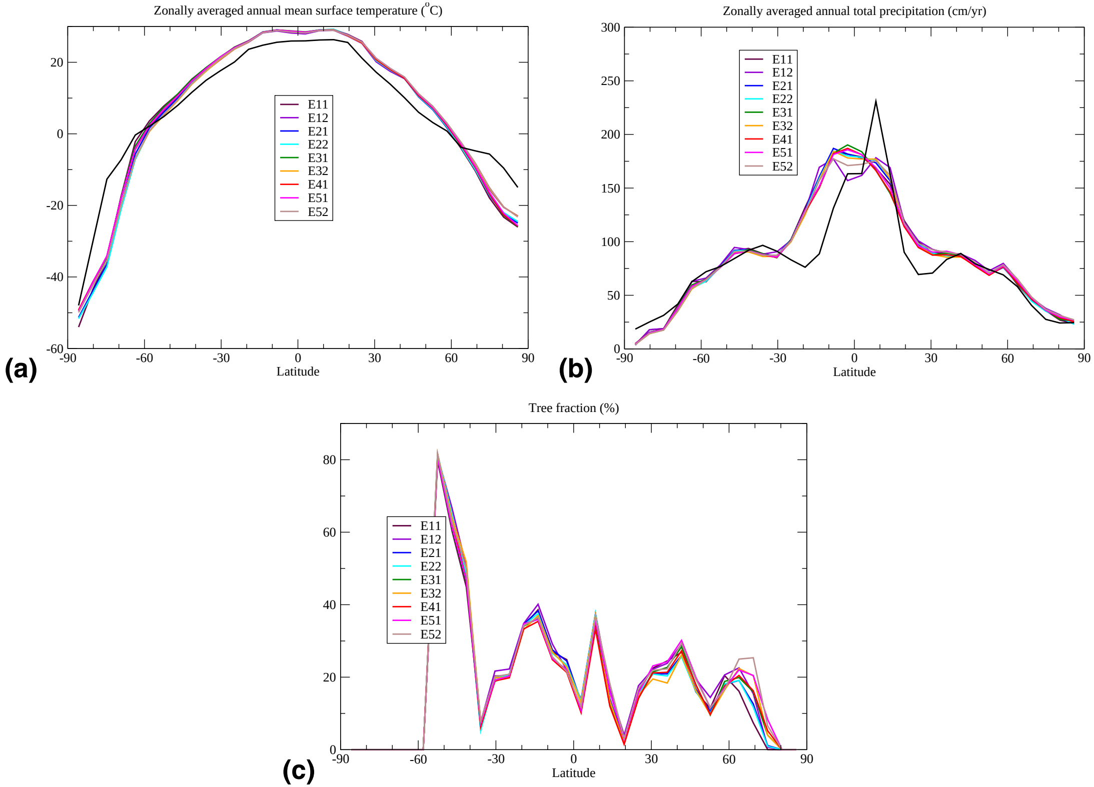

Fig. 1. Zonally averaged surface temperature (°C) **(a)**, annual mean precipitation (cm/yr) **(b)**, and tree fraction (%) **(c)** simulated for the pre-industrial time according to the nine climatic parameter sets (colour lines). Observations are in black (Brohan et al., 2006 for temperature; Xie and Arkin, 1996, 1997 for precipitation; http://www.monsoondata.org:9090/dods/gswp/grid/fixed/classfrac_igbp for tree fraction). Carbon parameter set 2 is used here.

CPD

6, 711–765, 2010

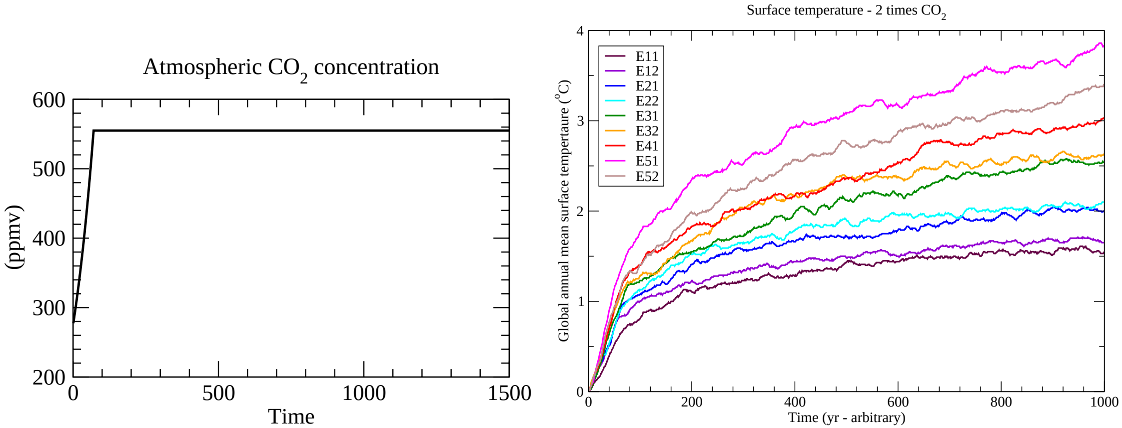

Fig. 2. Atmospheric CO_2 concentration in the perturbation scenario (left) and time evolution of the global annual mean surface temperature response to this perturbation according to the selected model parameter sets (right). Temperature is presented as deviation from the initial value.

CPD
6, 711–765, 2010

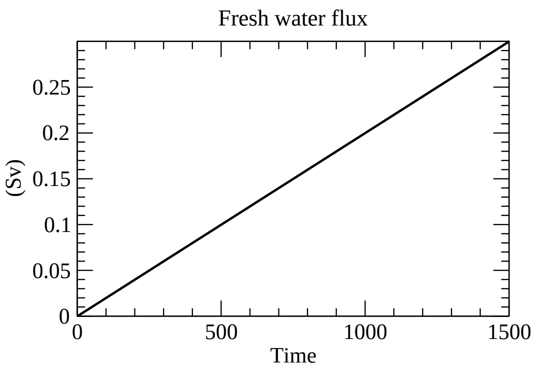

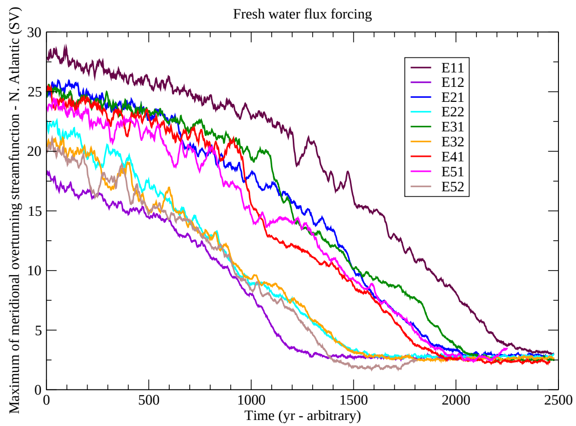

Fig. 3. Freshwater forcing in the North Atlantic in the perturbation scenario (left) and time evolution of the maximum of meridional overturning streamfunction below the Ekman layer in the Atlantic Ocean according to the selected model parameter sets in response to this perturbation (right). MOC is the absolute value.

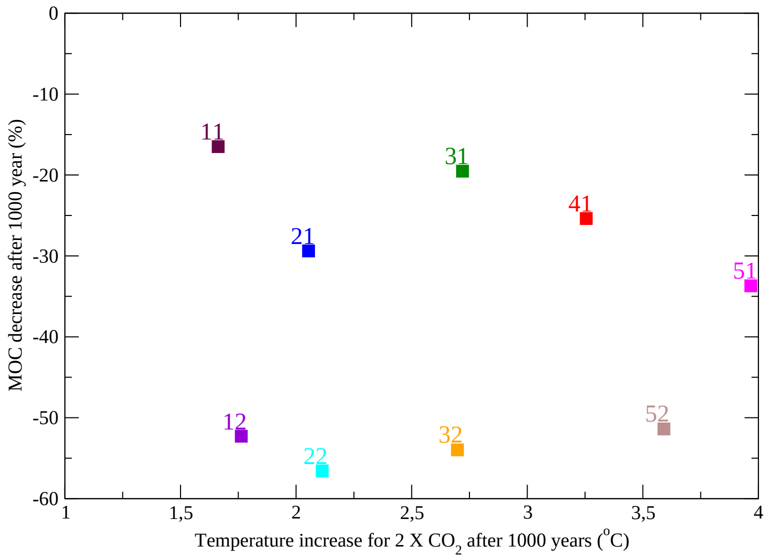

Fig. 4. Distribution of the model climatic parameter sets in the phase space (CO_2 sensitivity, MOC sensitivity).

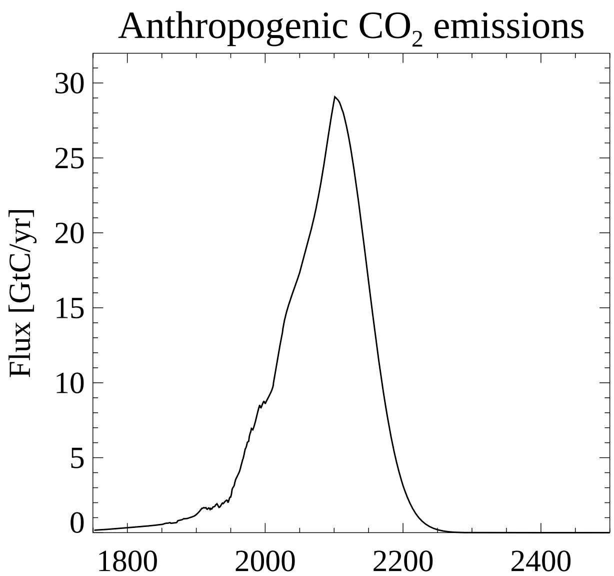

Fig. 5. CO_2 emission scenario used to assess the sensitivity of the carbon cycle to the different carbon parameter sets (see description of the scenario in the text). It includes both fossil fuel emission and fluxes related to land use change.

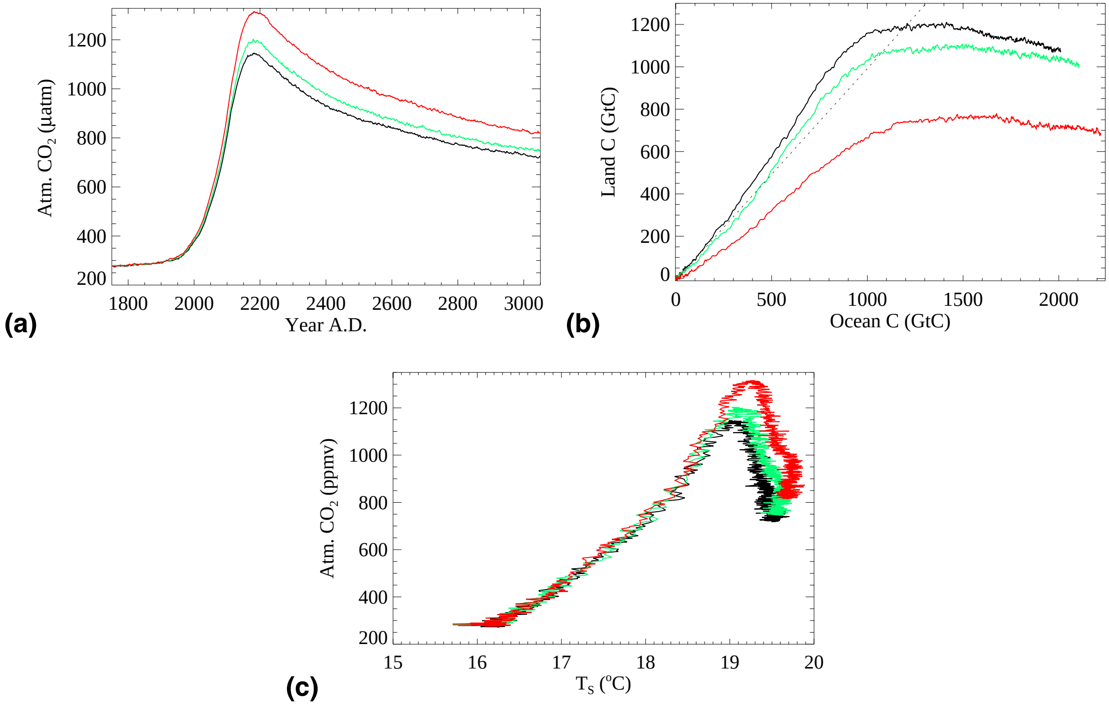

Fig. 6. Evolution of the annual mean atmospheric CO_2 concentration (ppmv) with time **(a)**, terrestrial carbon inventory versus ocean carbon inventory (both in GtC) **(b)** and atmospheric CO_2 vs. the global annual mean surface temperature **(c)** for the different carbon parameter sets. The dashed line in the panel **(b)** represents the 1:1 slope. Inventories are presented as anomalies with respect to the control run. The same color code is used in each panel, i.e. black for carbon parameter set 1, green for set 2 and red for set 3. Climatic parameter set 11 is used here.

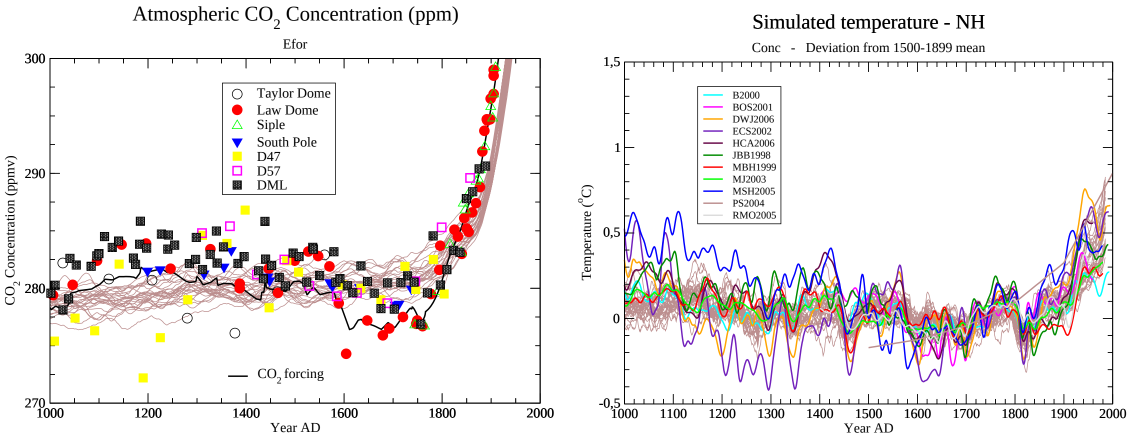

Fig. 7. Evolution of the atmospheric CO_2 concentration (ppmv) (left) and the Northern Hemisphere annual mean surface temperature (˚C) over the last millennium (in year AD) as simulated by LOVECLIM according to the 27 parameter sets (brown). Results are displayed for Efor-simulations in the case of the atmospheric CO_2 concentration and for Conc-simulations in the case of temperature. CO_2 concentration measured in Antarctic ice cores is shown for comparison. The full black line is the scenario of atmospheric CO_2 concentration used in the Conc-simulations. Temperatures are expressed as anomalies from their 1500 to 1899 means. They are smoothed with a 31-yr window. Temperature reconstructions using multiple climate proxy records (see Jansen et al., 2007 for details) are in colour lines. The individual series are identified in Table 4.

CPD
6, 711–765, 2010

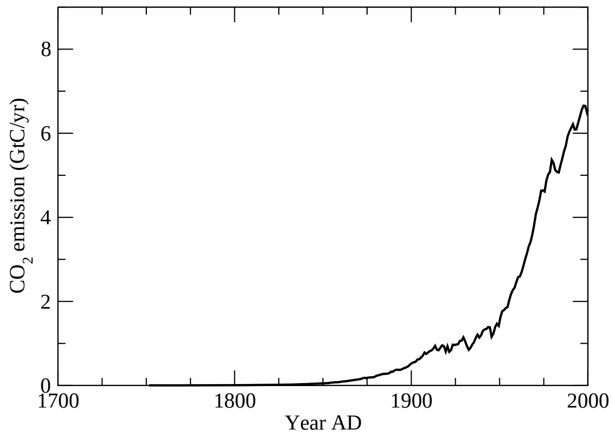

Fig. 8. Evolution over the last centuries (in year AD) of the emission of CO_2 (GtC/yr) from fossil fuel burning as prescribed in Efor simulations (Marland et al., 2003).

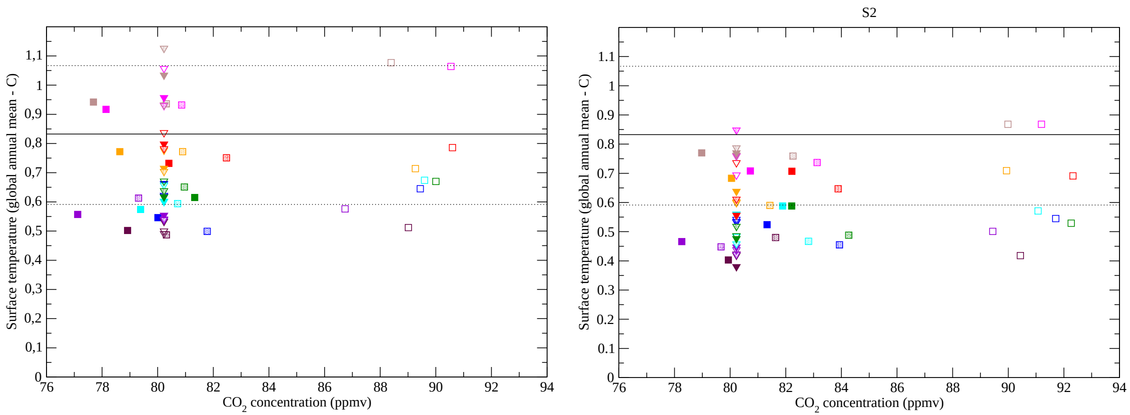

Fig. 9. Global annual mean surface temperature increase with respect to increase in atmospheric CO_2 concentration. The increase is computed between the beginning of the 20th century (mean value over 1901–1910) and the beginning of the 21st century (2000–2009). Values are averaged over five members of an ensemble. The left panel displays results for the S1 sulphate aerosol forcing. The sulphate aerosol forcing is doubled for the right panel (S2). Each colour corresponds to one set of climate parameters (see colour code in Fig. 4). Full symbols are for carbon parameter set 1, half-filled symbols are for carbon parameter set 2, and empty symbols are for carbon parameter set 3. Squares (triangles down) correspond to Efor (Conc) simulations. The vertical line of triangles representing the increase in atmospheric CO_2 concentration in the scenario used for Conc-simulations also represents the best observation-based estimate of this increase. The full black line indicates the temperature increase over the 20th century as reconstructed by Brohan et al. (2006) (i.e. 0.83 °C). The dashed lines are the upper and lower 95% uncertainty ranges.

CPD
6, 711–765, 2010

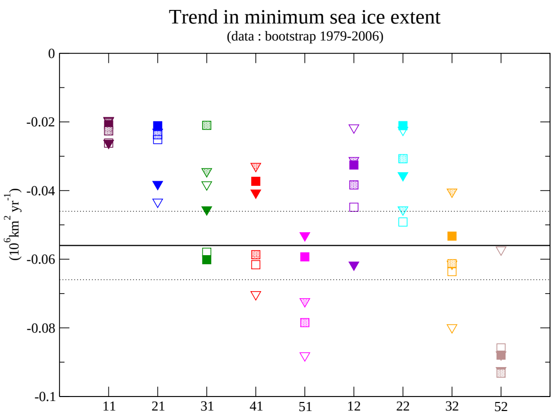

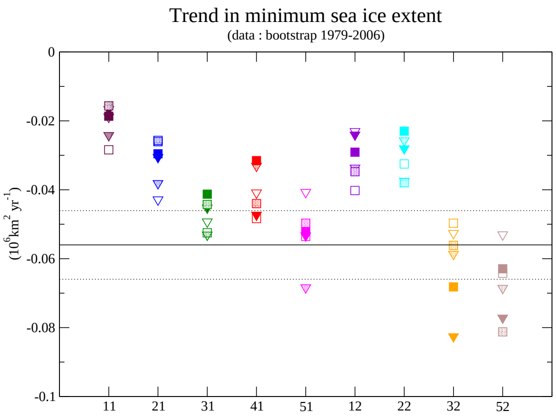

Fig. 10. Trend in minimum Northern Hemisphere sea ice extent between 1979 and 2006. X-axis is for the climate sensitivity, either for S1 (left) or S2 (right) sulphate aerosol forcing. Each colour corresponds to one set of climate parameters. Squares (triangles down) correspond to Efor (Conc) simulations; full symbols are for carbon parameter set 1, half-filled symbols are for carbon parameter set 2, and empty symbols are for carbon parameter set 3. The full black line indicates the minimum sea ice extent as reconstructed by Comiso and Nishio (2008). The dashed line represents the uncertainty related with the variability in the data (one standard deviation on the slope).

CPD
6, 711–765, 2010

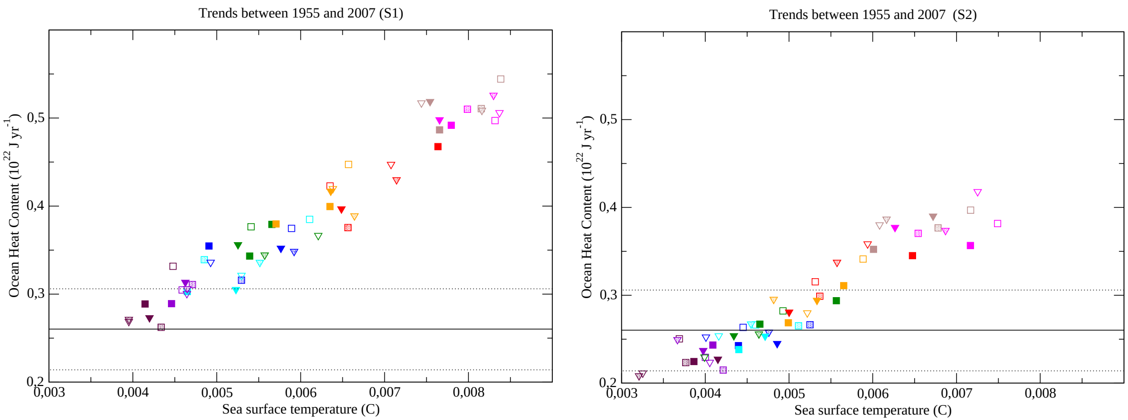

Fig. 11. Trend in ocean heat content in the upper 700 m (10^{22} J yr^{-1}) wrt trend in sea surface temperature (C yr^{-1}). Each symbol corresponds to one simulation, either for S1 (left) or S2 (right) sulphate aerosol forcing. Trends are computed as the slope of the regression line through the annual values between 1955 and 2007. Each colour corresponds to one set of climate parameters (see colour code in Fig. 4). Squares (triangles down) correspond to Efor (Conc) simulations; full symbols are for carbon parameter set 1, half-filled symbols are for carbon parameter set 2, and empty symbols are for carbon parameter set 3. The full black line represents the trend computed from observation (Levitus et al., 2009). The dashed line represents the uncertainty related with the variability in the data (one standard deviation on the slope of the linear regression through observation).

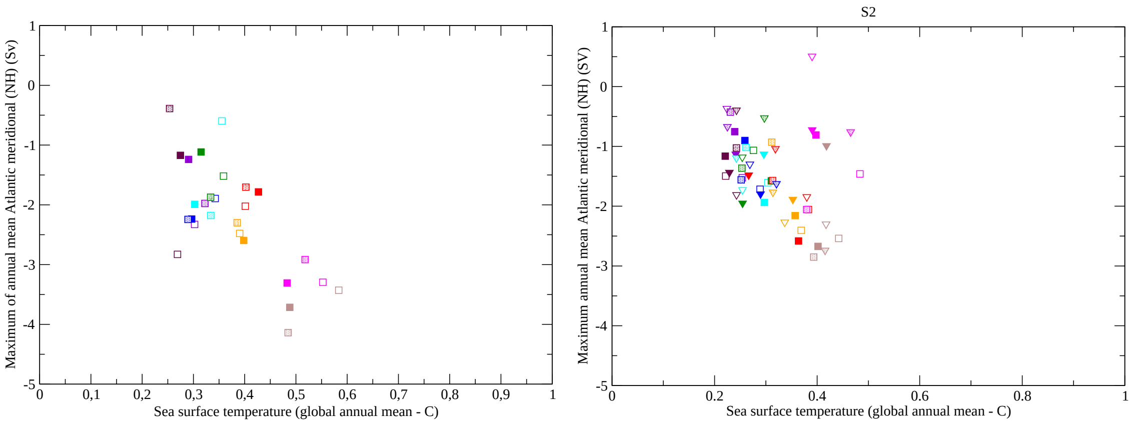

Fig. 12. Change in the maximum of the North Atlantic meridional overturning streamfunction (Sv) wrt to change in the global annual mean sea surface temperature (°C). Each colour corresponds to one set of climate parameters (see colour code in Fig. 4) either for S1 (left) or S2 (right) sulphate aerosol forcing. Squares (triangles down) correspond to Efor (Conc) simulations; full symbols are for carbon parameter set 1, half-filled symbols are for carbon parameter set 2, and empty symbols are for carbon parameter set 3.

CPD
6, 711–765, 2010

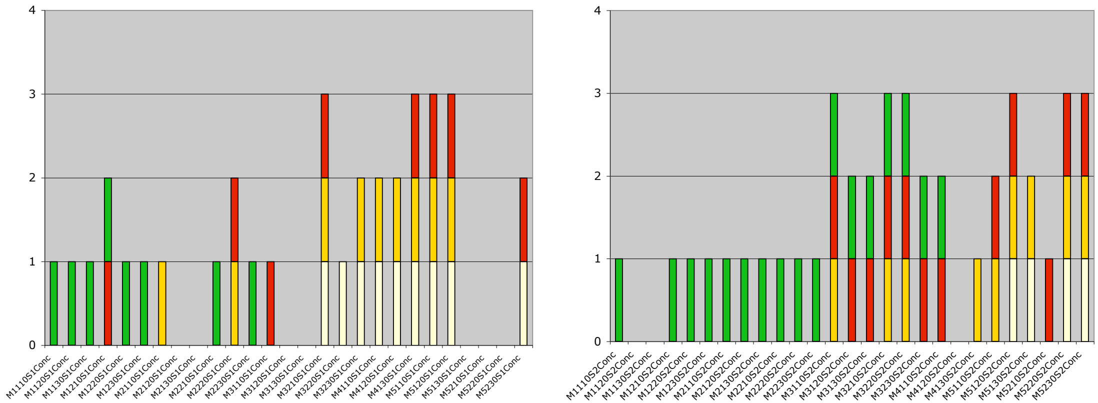

(a) (b)

Fig. 13. Summary of the performance of the Conc **(a, b)** and Efor **(c, d)** simulations to reproduce the observed trend of the time evolution for different climate variables for each parameter set under S1 **(a, c)** and S2 **(b, d)** sulphate aerosol forcings. The variables and the time intervals are described in Table 5. The x-axis lists all the parameter sets. Colour bars indicate the variables (see colour code) simulated with a good skill (according to our metric), i.e. R above the threshold (see text). A single colour bar is used for sea ice and upper ocean heat content. Ts stands for global annual mean surface temperature either over the interval 1901–2005 or 1979–2005. CO_2 is for atmospheric CO_2 concentration either over the time interval 1901–2005 or 1979–2005. Sea ice extent trend is computed either between 1979 and 2006 or 1979 and 2007. Trend in ocean heat content in the upper 700 m of the ocean is computed over either the time interval 1955–2007 or 1950–2003. See also Table 5 for references.

CPD
6, 711–765, 2010

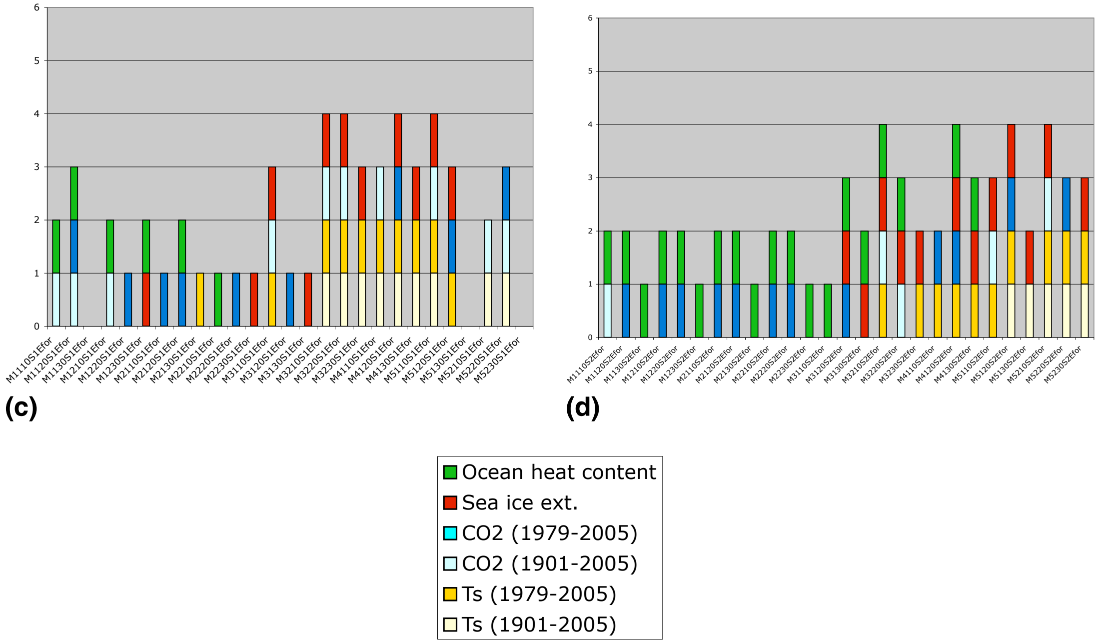

Fig. 13. Continued.

CPD
6, 711–765, 2010